Biennial report for Permanent Supersite/Natural Laboratory

Virunga Volcanoes Supersite Biennial Report: 2024- 2025

History	***http://geo-gsnl.org/supersites/permanent-supersites/virunga-supersite/***
Supersite Coordinator	*Charles Balagizi* *Goma Volcano Observatory* *142, Avenue du Rond-Point,* *Quartier des Volcans,* *Goma City, Democratic Republic of the Congo* *Email : balagizi.charles@gmail.com* *Cell & WhatsApp: +243 975803568*

1. Abstract

Data collected in 2024 and 2025 reveal that the tectonic framework of the Kivu segment was controlled by extensional faulting associated with continental rifting, resulting in frequent earthquakes from both tectonic processes and volcanic activity. Analysis of seismicity between during the study period shows that most earthquakes occurred at shallow depths, generally between 0 and 15 km, with magnitudes typically ranging from Mw 1.0 to Mw 4.0. Spatial distribution patterns reveal clusters of earthquakes along major rift faults and around southern Lake Kivu. Temporal analysis indicates persistent background seismicity with occasional peaks in activity, reflecting continuous crustal deformation driven by tectonic extension and magma movement beneath the Virunga volcanic field. Measurements of gas emissions, particularly sulfur dioxide (SO_2) and carbon dioxide (CO_2), provide important indicators of magma dynamics beneath Nyiragongo and Nyamulagira volcanoes. Data collected using both DOAS instrument that from the satellite indicate that Nyiragongo experienced intense degassing activity during 2024 and 2025, with SO_2 flux peaks exceeding 11,000 tons per day. These elevated emissions suggest increased magmatic activity within the volcanic conduit system following the Nyiragongo May 2021 eruption. Soil-CO_2 emissions measurements conducted in and around war displaced persons camps near Goma city indicated that most camp areas presented low to middle risk, nevertheless, surrounding zones exhibited extremely high concentrations exceeding 15%, which represent potentially lethal conditions. These results emphasize the importance of hazard mapping, public awareness, and mitigation measures such as warning signs and regular monitoring campaigns. Satellite remote sensing techniques played an essential role in monitoring volcanic activity and ground deformation. In fact, SAR data were used to analyze deformation patterns at Nyiragongo and Nyamulagira volcanoes, revealing subsidence trends inside the craters, and evidence of regular lava overflowing Nyamulagira crater with directions in the Virunga National Park. Satellite observations also indicate progressive infilling of the Nyiragongo crater following the drainage of its lava lake during the May 2021 eruption. In addition to volcanic monitoring, geochemical data was collected in lake Kivu and contribute to the understanding of the lake stratification and stability, as well as providing a baseline information regarding water quality. During 2024 and 2025, 3 Goma volcano Observatory researchers spent year at INGV, being trained in GNSS, satellite and geochemical data collection, processing and interpretation. The findings of Virunga Supersite during 2024 and 2025 highlight the importance of integrating ground-based and satellite observations to provide a comprehensive approach to understanding Virunga volcanoes complex systems and improving hazard assessment for the millions of people living around Nyiragongo and Nyamulagira volcanoes, particularly those in Goma city. Continued monitoring and international scientific collaboration are therefore essential to mitigate potential risks associated with volcanic and tectonic activity. However, monitoring efforts were partially disrupted in early 2025 due to the vandalization of the Rusayo and Sake DOAS stations, also the GNSS and MultiGAS donated by the GEO-GSNL and the VDAP, respectively could not be deployed because of the insecurity in the field. These are examples of several difficulties of the logistical challenges associated with scientific monitoring of active volcanoes in areas affected by regional insecurity.

2. Scientists/science teams

Charles Balagizi	***Geochemistry Department,*** ***Goma Volcano Observatory. 142, Avenue du Rond-Point, Quartier des Volcans, Goma City, Democratic Republic of the Congo*** ***balagizi.charles@gmail.com*** ***https://www.researchgate.net/profile/Charles_Balagizi***
Arsène T. Sadiki	*Department of Seismology, Goma Volcano Observatory* *142, Avenue du Rond-Point, Quartier des Volcans, Goma City, Democratic Republic of the Congo* *sadikiarsenetb@gmail.com*
Honoré Ciraba	*Department of Geodesy, Goma Volcano Observatory* *142, Avenue du Rond-Point, Quartier des Volcans, Goma City, Democratic Republic of the Congo* *honoreciraba@yahoo.fr*
King Iragi	*Department of Geodesy, Goma Volcano Observatory* *142, Avenue du Rond-Point, Quartier des Volcans, Goma City, Democratic Republic of the Congo* *iragiking7@gmail.com*
Jonathan Kavuke	*Department of Geodesy, Goma Volcano Observatory* *142, Avenue du Rond-Point, Quartier des Volcans, Goma City, Democratic Republic of the Congo* *jkavuke@gmail.com*
Sandra Nzamu	*Department of Geodesy, Goma Volcano Observatory* *142, Avenue du Rond-Point, Quartier des Volcans, Goma City, Democratic Republic of the Congo* *sandynzamu@gmail.com*
Bonheur Ngangu	*Department of Geodesy, Goma Volcano Observatory* *142, Avenue du Rond-Point, Quartier des Volcans, Goma City, Democratic Republic of the Congo* *bonheurrugain@gmail.com*
Niche Mashagiro	*Department of Technics, Goma Volcano Observatory* *142, Avenue du Rond-Point, Quartier des Volcans, Goma City, Democratic Republic of the Congo* *nichemashagiro@gmail.com*
Marcellin Kasereka	*Geochemistry Department,* *Goma Volcano Observatory. 142, Avenue du Rond-Point, Quartier des Volcans, Goma City, Democratic Republic of the Congo* *marcellinkasereka16@gmail.com*
Mathieu Yalire	*Geochemistry Department,* *Goma Volcano Observatory. 142, Avenue du Rond-Point, Quartier des Volcans, Goma City, Democratic Republic of the Congo* *yaliremat@yahoo.fr*
Bo Galle	*Chalmers University of Technologie,* **Hörsalsvägen 11, Floor 4** *bo.galle@chalmers.se* *http://www.chalmers.se/en/Pages/default.aspx*
Michael Poland	*U.S. Geological Survey, Cascades Volcano Observatory* *1300 SE Cardinal Court, Suite 100* *Vancouver, WA 98683* *mpoland@usgs.gov* *https://www.usgs.gov/staff-profiles/michael-poland*

Marcello Liotta	*Istituto Nazionale di Geofisica e Vulcanologia* *Via Ugo La Malfa, 153* *90146 - Palermo (Italy)* *marcello.liotta@ingv.it* *https://sites.google.com/ingv.it/marcello-liotta/*
Yosuke Aoki	*Earthquake Research Institute, University of Tokyo* *1-1 Yayoi 1, Bunkyo-ku- Tokyo* *113-0032, Japan* *yaoki@eri.u-tokyo.ac.jp* *http://www.eri.u-tokyo.ac.jp*
Gaetana Ganci	*Istituto Nazionale di Geofisica e Vulcanologia* *Piazza Roma, 2 - 95125 Catania* *gaetana.ganci@ingv.it*
Annalisa Cappello	*Istituto Nazionale di Geofisica e Vulcanologia* *Piazza Roma, 2 - 95125 Catania* *annalisa.cappello@ingv.it*
Cristina Proietti	*Istituto Nazionale di Geofisica e Vulcanologia* *Piazza Roma, 2 - 95125 Catania* *cristina.proietti@ingv.it*
Sven Borgstrom	*Istituto Nazionale di Geofisica e Vulcanologia,* *Vesuviano Observatoy, Italia* *sven.borgstrom@ingv.it*
Mario Mattia	*Istituto Nazionale di Geofisica e Vulcanologia* *Piazza Roma, 2 - 95125 Catania-Italia* *mario.mattia@ingv.it*
Eugenio Privitera	*Istituto Nazionale di Geofisica e Vulcanologia* *Piazza Roma, 2 - 95125 Catania-Italia* *eugenio.privitera@ingv.it*
Mauro Coltelli	*Istituto Nazionale di Geofisica e Vulcanologia* *Piazza Roma, 2 - 95125 Catania* *mauro.coltelli@ingv.it*
Sebastien Valade	*Universidad Nacional Autónoma de México* *Instituto de Geofísica* *valade@igeofisica.unam.mx*
Diego Coppola	*Dipartimento di Scienze della Terra, Università degli Studi di Torino* *TORINO, Italia* *diego.coppola@unito.it*
Cristiano Tolomei	*Istituto Nazionale di Geofisica e Vulcanologia* *Osservatorio Nazionale Terremoti* *Via di Vigna Murata 605, 00143 Rome, Italy* *cristiano.tolomei@ingv.it*
Lisa Beccaro	*Istituto Nazionale di Geofisica e Vulcanologia* *Osservatorio Nazionale Terremoti* *Via di Vigna Murata 605, 00143 Rome, Italy* *lisa.beccaro@ingv.it*
Silvia Puliero	*Istituto Nazionale di Geofisica e Vulcanologia* *Osservatorio Nazionale Terremoti* *Via di Vigna Murata 605, 00143 Rome, Italy*
Emanuele Ferrentino	*Istituto Nazionale di Geofisica e Vulcanologia* *Osservatorio Nazionale Terremoti* *Via di Vigna Murata 605, 00143 Rome, Italy* *emanuele.ferrentino@ingv.it*

Marco Polcari	*Istituto Nazionale di Geofisica e Vulcanologia* *Osservatorio Nazionale Terremoti* *Via di Vigna Murata 605, 00143 Rome, Italy* *marco.polcari@ingv.it*
Elisa Trasatti	*Istituto Nazionale di Geofisica e Vulcanologia* *Osservatorio Nazionale Terremoti* *Via di Vigna Murata 605, 00143 Rome, Italy* *elisa.trasatti@ingv.it*

Scientists/science teams issues

The participation of local scientists in the processing and interpretation of ground-based and Earth Observation and data has been improved once again, this is a result of training undertaken abroad, particularly at INGV Roma and Catania. As an example, the section of the present report related to seismology has been strictly prepared by a local scientist, data processing and interpretation included. Nevertheless, important capacity gaps still remain, also the capacities of local technicians to deploy and maintain instruments have to be improved. To address these limitations and further strengthen local expertise, the continuation of hybrid training programs combining international and local learning components will be essential to enhance the technical and analytical capacities of local scientists and technicians.

3. In situ data

Type of data	Data provider	How to access	Type of access
Seismic	*Goma Volcano Observatory (GVO)*	*Published papers* Contact GVO***	*Unregistered Public*
GPS	*GVO*	*Contact GVO***	*GSNL scientists*
Gas measurements	*GVO*	*Published papers* Contact GVO***	*Unregistered Public GSNL scientists*
Surface waters chemistry including Lake Kivu	*GVO*	*Published papers* Contact GVO***	*Unregistered Public GSNL scientists*
Rainwater chemistry	*GVO*	*Published papers* Contact GVO***	*Unregistered Public GSNL scientists*

**Published data are freely accessible; the Goma Volcano Observatory may be contacted for guidance in case of issues*

***Archived unpublished data or recently collected data are available on request, and based on the data policy for data sharing and management among the Virunga Supersite scientific community.*

In situ data issues

- Some instruments were note deployed because of the insecurity in the field around Nyiragongo and Nyamulagira volcanoes, they include 5 GNSS donated by the GEO GNSS as well as a MultiGAS station donated by the VDAP.
- Available data can be accessed following this data policy, http://geo-gsnl.org/wp-content/Documents/Supersites/Virunga/History/Virunga%20Supersite_Data%20Policy.pdf

4. Satellite data

Type of data	Data provider	How to access	Type of access
COSMO-SkyMed	*ASI*	*POC requests access from ASI for GSNL scientists individual users, data is then accessible* over ASI Server facilities following dedicated instructions from ASI.	*GSNL scientists*
Pleiades	*CNES*	*POC requests access from CNES for individual users*	*GSNL scientists*
Sentinel-1 a/b	*ESA*	*https://scihub.copernicus.eu/*	*Registered public*
ASTER ***EO-1 (Hyperion)*** ***MODIS***	*NASA*	*https://terra.nasa.gov/about/terra-instruments/modis* *https://modis.gsfc.nasa.gov/*	*Registered public*
Landsat	*USGS*	*https://www.usgs.gov/land-resources/nli/landsat/landsat-data-access?qt-science_support_page_related_con=0#qt-science_support_page_related_con*	*Registered public*
AVHRR	*NOAA*	https://earth.esa.int/web/guest/missions/3rd-party-missions/current-missions/noaa-avhrr	*Registered public*
SAOCOM 1	*CONAE*	https://catalog.saocom.conae.gov.ar/catalog/#/	*GSNL scientists*

Satellite data issues

We continue having problems in acquiring Pléiades imagery over the Virunga volcanoes with minimal cloud cover, while these imageries are strongly needed to produce a new DEM over the active volcanoes and the city of Goma and other small towns and villages.

5. Research results

5.1. In situ data

5.1.1. Seismicity of the Virunga Volcanic Province

a. Introduction

The Kivu Rift forms a key segment of the western branch of the East African Rift System (EARS), straddling the eastern Democratic Republic of Congo (DRC) and western Rwanda. It is characterized by a complex system of active half-grabens bounded by normal faults, which reflect ongoing crustal extension and lithospheric thinning (Ebinger and Scholz, 2011). The Lake Kivu Basin constitutes a transition zone of the WRA from the predominant northwesterly orientation of the Rusizi - Tanganyika Rift Basin to the more southwest to the northeast trend of the Lake Kivu, Virunga, and Rutchuru - Lake Edouard Rift Basins (Ebinger, 1989). The NE-SW faults dominate the Lake Kivu region. They belong to the Mesoproterozoic Karagwe-Ankole Belt and are overprinted, to the west of Lake Kivu, by NNE - SSW faults of the Neoproterozoic Itombwe Synclinorium which reoriented the rift direction (Villeneuve, 1987; Villeneuve and Chorowicz, 2004). This zone has experienced moderate to large earthquake (e.g The 24 October Kalehe earthquake Mw6.2; the 03 February 2008 Bukavu - Cyangugu earthquake Mw6.0; the 07 August 2015 Katana earthquake Mw5.8). These earthquakes claimed lives; more people were injured, and caused some houses to collapse (d'Oreye et al., 2011; Mavonga, 2007; Mavonga and Durrheim, 2009; Tuluka et al., 2020).

The rift is notable for intense volcanic activity, dominated by Nyiragongo and Nyamulagira, two of the most active volcanoes in Central Africa. These volcanoes are located within a structurally controlled volcanic field influenced by both the regional fault system and deep magmatic plumbing potentially linked to a mantle plume component beneath the Virunga Volcanic Province (Smets et al., 2015). The interaction between tectonic deformation and magmatism has led to complex fault volcano relationships, such as dyke-induced faulting, which can trigger both volcanic and tectonic earthquakes (Mavonga et al., 2010).

The rift also hosts Lake Kivu, a deep, meromictic lake that overlies an active tectonic graben and contains exceptionally large volumes of dissolved gases, primarily carbon dioxide (CO_2) and methane (CH_4). The accumulation of these gases in the lake's bottom layers is driven by volcanic and hydrothermal inputs through fault zones beneath the lake floor. This poses a rare but catastrophic natural hazard known as a limnic eruption, as demonstrated by the 1986 Lake Nyos disaster in Cameroon (Halbwachs et al., 2002). However, the presence of methane also represents a potential energy resource, attracting interest in controlled gas extraction while raising concerns over environmental and human safety (Balagizi et al., 2018b; Darchambeau et al., 2014). Geodynamical, the Kivu Rift is situated in a transitional zone between the Albertine Rift to the north and the Rungwe Volcanic Province to the south. Its evolution is governed by a combination of active faulting, volcanism, and the reactivation of inherited Proterozoic basement structures, particularly those associated with the Ubende and Kibaran belts (Delvaux et al., 2017). These inherited fabrics often localize modern faulting and influence magma migration pathways, making the tectonic architecture of the region unusually complex.

The region experiences frequent seismic activity, including both tectonic earthquakes due to extensional faulting and volcano-tectonic events linked to magma movement beneath the active volcanoes (Mavonga et al., 2010). Earthquake swarms are commonly observed in association with dyke intrusions or gas migration episodes and can occur along previously unidentified faults, underscoring the need for high-resolution geophysical monitoring.

Due to this convergence of tectonic deformation, active magmatism, and gas-rich hydrogeology, the Kivu Rift represents a unique natural laboratory for the study of continental rifting, intraplate volcanism, and gas-charged lacustrine systems(Balagizi et al., 2018b; Darchambeau et al., 2014; Delvaux et al., 2017; Ebinger and Scholz, 2011).

b. Seismicity of the Virunga between January and June 2024

Between January and June 2024, seismicity in the western branch of the East African Rift System was dominated by shallow, low-to-moderate magnitude earthquakes distributed along major rift structures. Spatial and temporal patterns (Figures 1-A&B) show persistent activity concentrated in the Kivu Rift, with most events occurring at depths of 0 -12 km and magnitudes ranging from Mw 1.0 to 4.0.

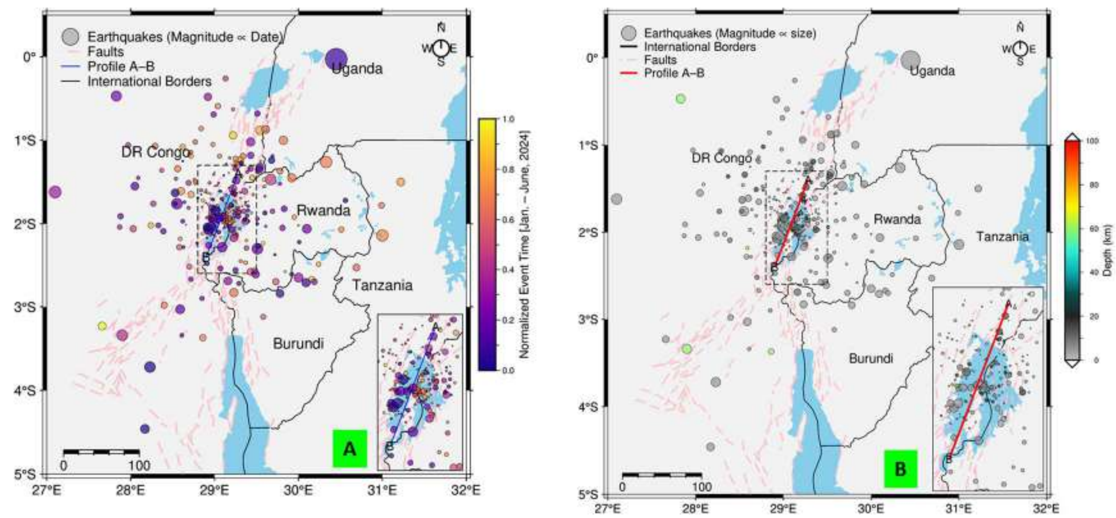

Figure 1. *(A) Spatial Distribution and Temporal Evolution of Earthquakes in the Western Branch of the East African Rift (January to June, 2024). (B) Earthquake Depth Distribution and Magnitude in the Western Branch of the East African Rift (January to June, 2024).*

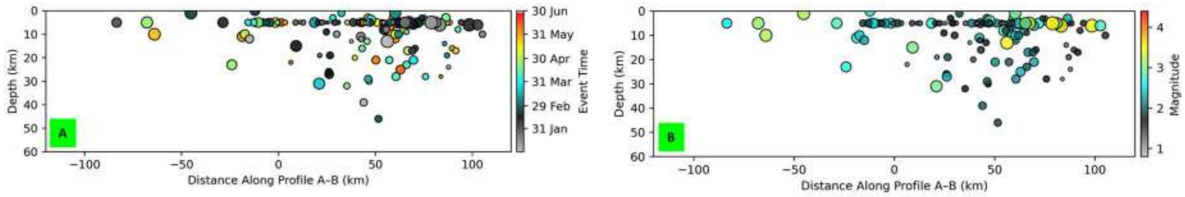

Figure 2. (A) Cross-Section of Earthquake Hypocenter along Profile A–B in the Virunga volcanic Province, Western Branch of the East African Rift from January to June, 2024. (B) Spatio-temporal Distribution of Earthquake Depths along Profile A – B in the Virunga volcanic Province, Western Branch of the East African Rift from January to June, 2024.

Cross-sections along profile A - B (Figures 2) reveal that hypocenters are clustered within the upper crust, with clear depth layering and localized zones of repeated activity. Magnitude - depth relationships (Figure 3) indicate that the largest events are confined to very shallow depths (<8 km), increasing their potential surface impact despite moderate magnitudes. Daily seismicity rates remained variable but showed sustained background activity throughout the six-month period (Figure 4).

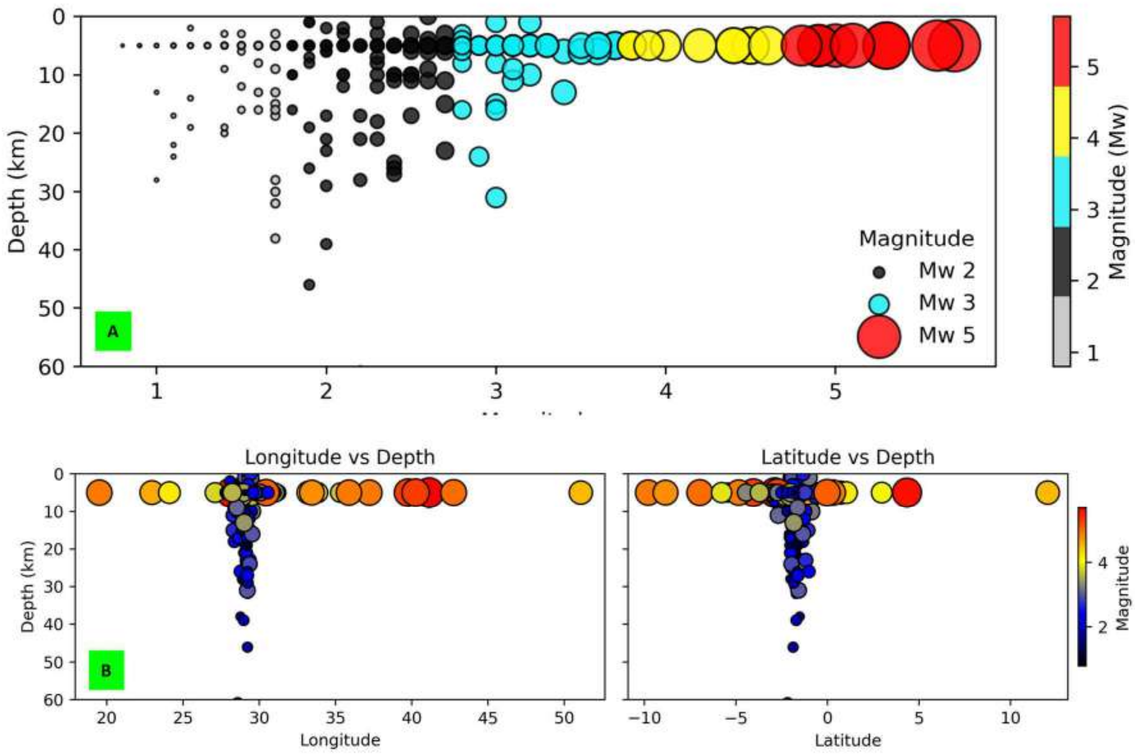

Figure 3. (A) Earthquake magnitude vs. depth in the Virunga Volcanic Province, Western Branch of the East African Rift from January to June, 2024. Circle size scales with event magnitude. Most high-magnitude events (yellow to red) are confined to < 8 km depth. (B) Depth variation of earthquakes plotted against longitude (left) and latitude (right). Circle size scales with magnitude, and colour represents magnitude using a black-to-red gradient.

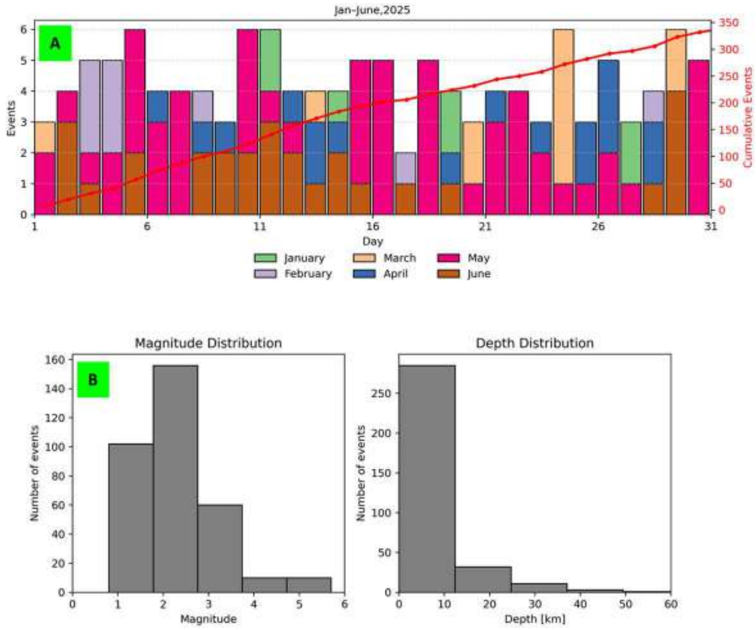

Figure 4. Daily earthquake counts for January to June, 2024 and cumulative count over the 6-month period (red line). Histograms showing the distribution of earthquake magnitudes (left) and focal depths (right) from January to June, 2024. Most events are shallow (0 - 12 km) and low magnitude (Mw 1.0 – 4.0).

Kernel density mapping (Figure 5) highlights distinct seismicity hotspots that align with mapped faults and border regions around Lake Kivu, suggesting that ongoing tectonic extension potentially influenced by magmatic processes continues to drive crustal deformation in the area.

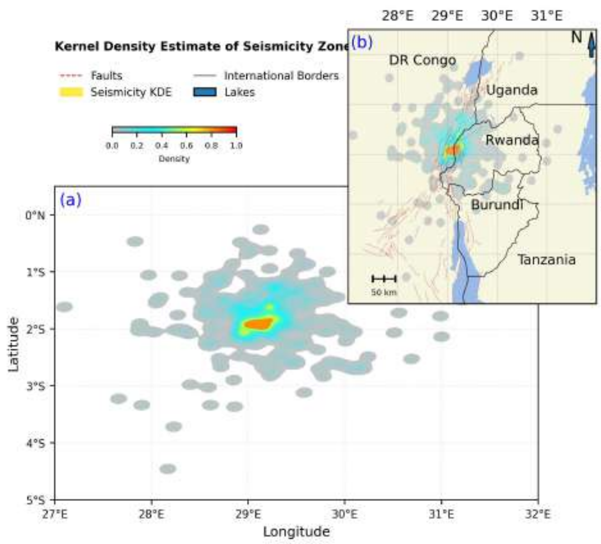

***Figure 5. (A)** Kernel density estimate (KDE) map of seismicity from January to June, 2024, normalized to maximum density. **(B)** Overlay of seismicity KDE on a geographic base map showing regional fault traces and international borders. (Processed data is from the Western Branch of the East African Rift from January to June, 2024).*

c. Seismicity of the Virunga between July and December 2024

Between July and December 2024, seismicity in the Kivu Rift region was characterized by a clear concentration of earthquakes along the western branch of the East African Rift System, particularly around southern Lake Kivu near the DRC and Rwanda border (Figure 6).

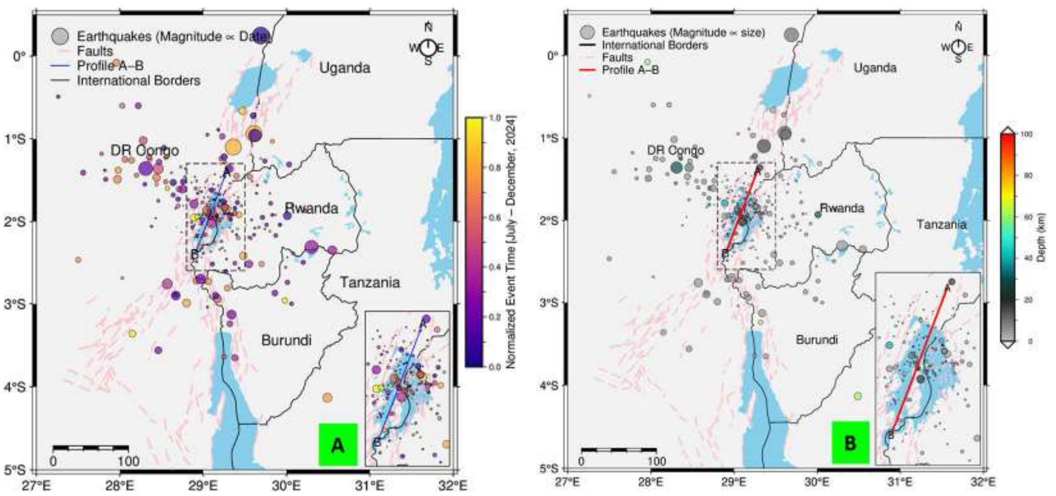

Figure 6. *(A) Spatial Distribution and Temporal Evolution of Earthquakes in Virunga Volcanic Province, Western Branch of the East African Rift from July to December 2024. (B) Earthquake Depth Distribution and Magnitude in in Virunga Volcanic Province, Western Branch of the East African Rift from July to December 2024.*

Depth profiles show that the majority of events occurred in the brittle upper crust, mostly above 5 km, with a strong cluster shallower than 10 km (Figure 7).

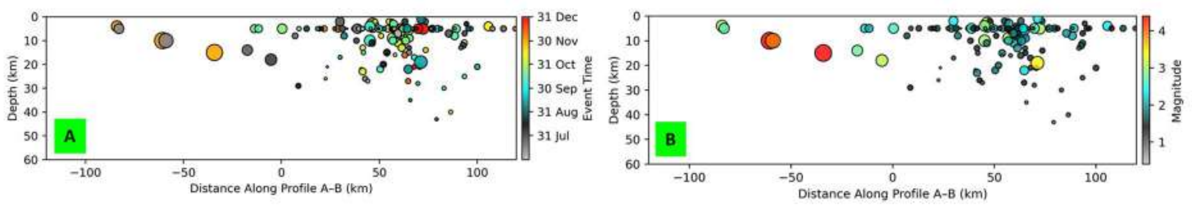

Figure 7*. (A) Cross-Section of Earthquake Hypocenters along Profile A – B in Virunga Volcanic Province, Western Branch of the East African Rift from July to December 2024. (B) Spatio-temporal Distribution of Earthquake Depths along Profile A – B in Virunga Volcanic Province, Western Branch of the East African Rift from July to December 2024.*

Magnitude analyses indicate that seismicity was dominated by low-to-moderate events (Mw 1.0–3.5), although occasional larger earthquakes (>Mw 4.5) were also recorded. Notably, the larger events tended to be shallow, increasing their potential surface impact despite moderate magnitudes (Figure 8).

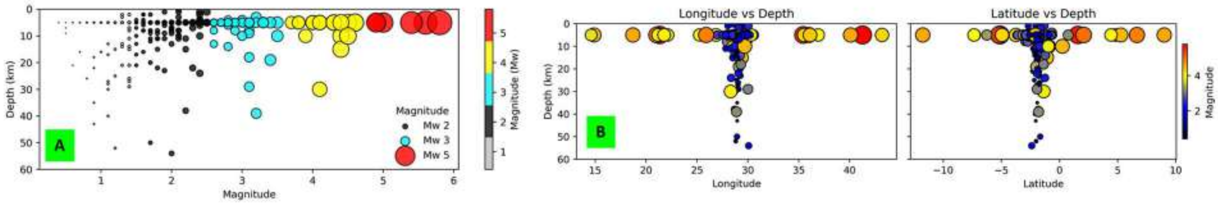

Figure 8. *(A) Earthquake magnitude vs. depth in Virunga Volcanic Province, Western Branch of the East African Rift from July to December 2024. Circle size scales with event magnitude. Most high-magnitude events (yellow to red) are confined to <20 km depth. (B) Depth variation of earthquakes plotted against longitude (left) and latitude (right) in Virunga Volcanic Province, Western Branch of the East African Rift from July to December 2024. Circle size scales with magnitude, and color represents magnitude using a black-to-red gradient.*

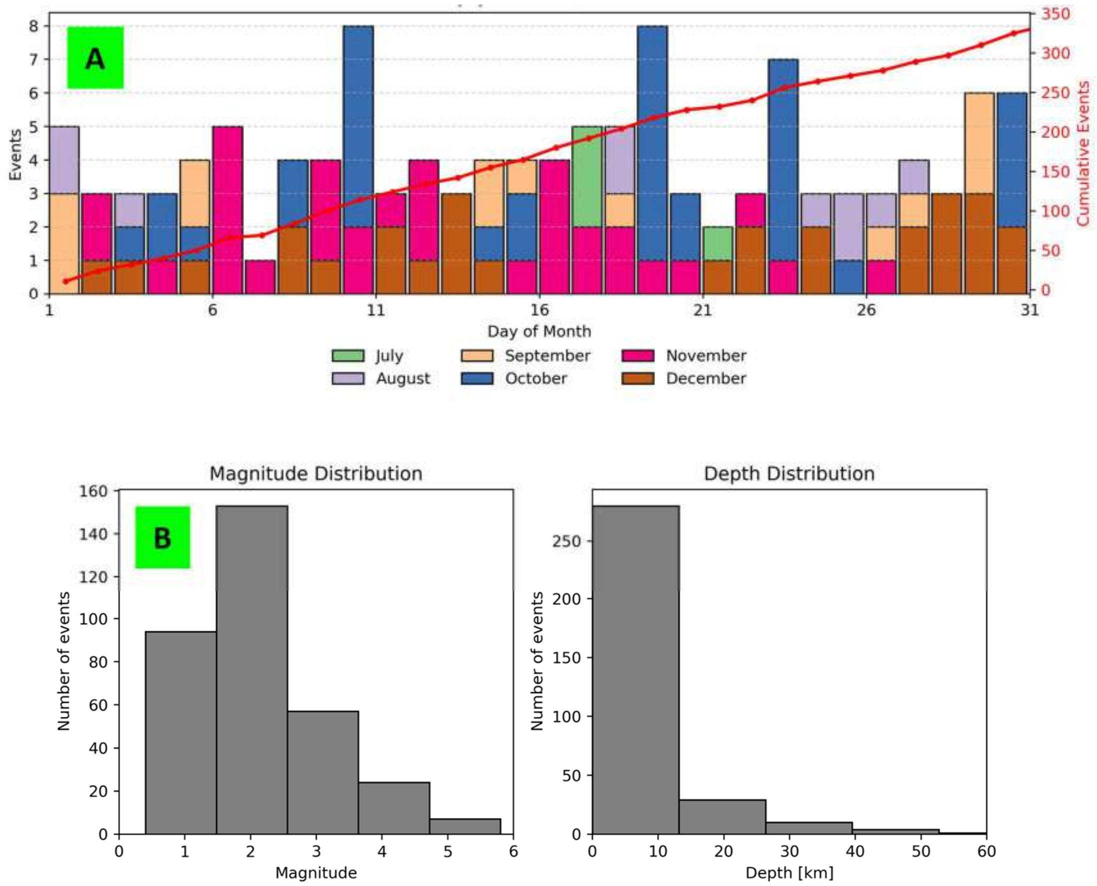

Figure 9. *(A) Daily earthquake counts from July to December 2024 and cumulative count over the 6-month period (red line) in the Virunga Volcanic Province, Western Branch of the East African Rift. (B)* Histograms showing the distribution of earthquake magnitudes (left) and focal depths (right) *in the Virunga Volcanic Province, Western Branch of the East African Rift from July to December 2024*. Most events are shallow (0 - 12 km) and low magnitude (Mw 1.0 – 3.5).

Kernel density estimation highlights a pronounced seismicity hotspot near Goma and Bukavu, overlapping both active rift faults and densely populated areas an alignment that elevates regional hazard levels (Figure 10). The spatial distribution and depth - magnitude patterns together point to ongoing crustal deformation driven by a combination of tectonic extension and magmatic processes. These findings underscore the importance of sustained real-time monitoring and integrated geophysical studies to refine hazard assessments in the Kivu Rift.

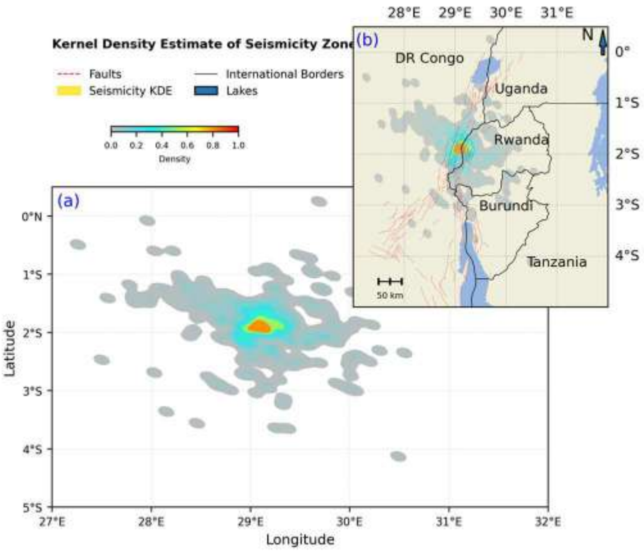

Figure 10. Kernel density estimate (KDE) map of seismicity from July to December 2024 in the Virunga Volcanic Province, Western Branch of the East African Rift from July to December 2024, normalized to maximum density. (b) Overlay of seismicity KDE on a geographic base map showing regional fault traces and international borders.

d. Seismicity patterns and tectonic context in the Virunga between April and June 2025

The spatial distribution of seismicity observed between April and June 2025 highlights a strong concentration of earthquakes along the western branch of the East African Rift System (EARS), particularly in the Kivu Rift region (Figure 11).

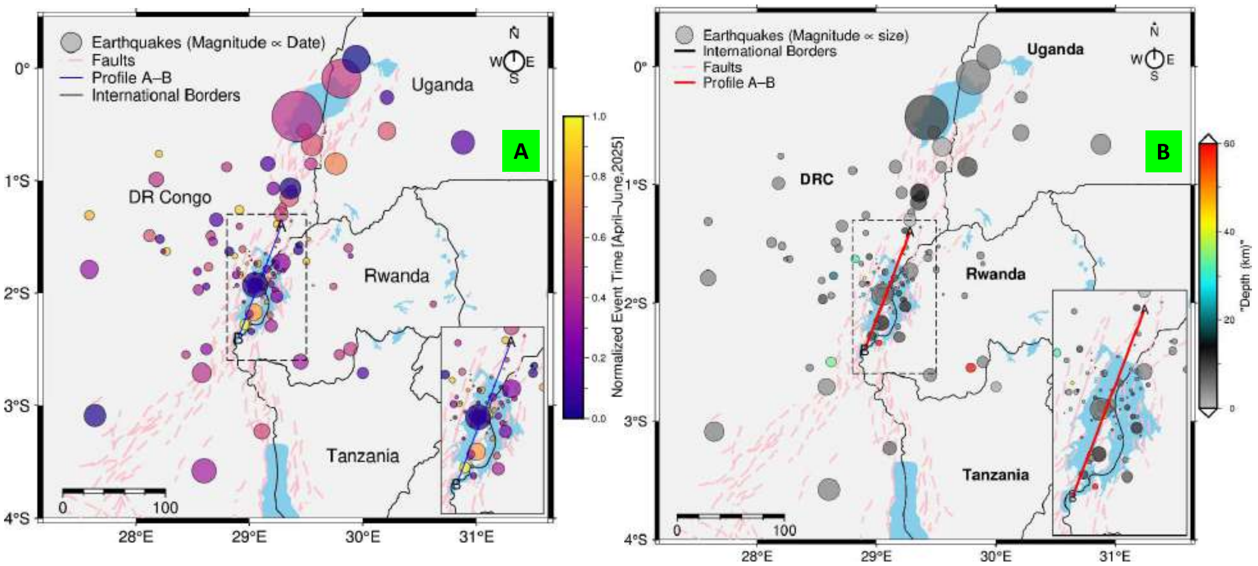

Figure 11. (A) Spatial Distribution and Temporal Evolution of Earthquakes in the Western Branch of the East African Rift (April - June 2025). (B) Earthquake Depth Distribution and Magnitude in the Western Branch of the East African Rift (April - June 2025)

Most epicenters align closely with known fault systems and rift-parallel structures, suggesting a strong tectonic control on earthquake occurrence. The depth distribution of events along profile A - B (Figures 12) confirms that most earthquakes are confined to the upper crust, predominantly above 15 km. This is typical of extensional rift settings where brittle failure dominates.

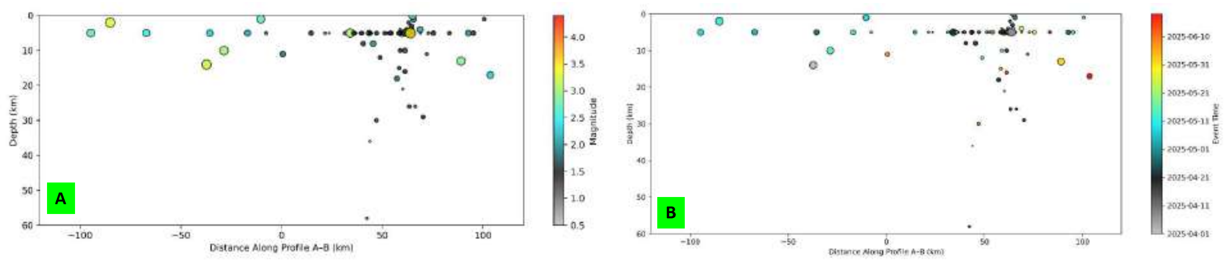

Figure 12. (B) Cross-Section of Earthquake Hypocenters along Profile A–B, (B) Spatio-temporal Distribution of Earthquake Depths along Profile A – B in the Virunga Volcanic Province, Western Branch of the East African Rift from April to June 2025.

- **Depth and magnitude characteristics**

Depth vs. magnitude analysis (Figure 13) reveals that most earthquakes occurred at shallow depths, generally less than 15 km, with few deeper than 30 km. This depth range is consistent with the brittle upper crust, where extensional faulting is most effective. The majority of events were of low-to-moderate magnitude, with a significant number clustering between Mw 1.0 and Mw 3.0, although some larger events exceeding Mw 4.5 were also recorded.

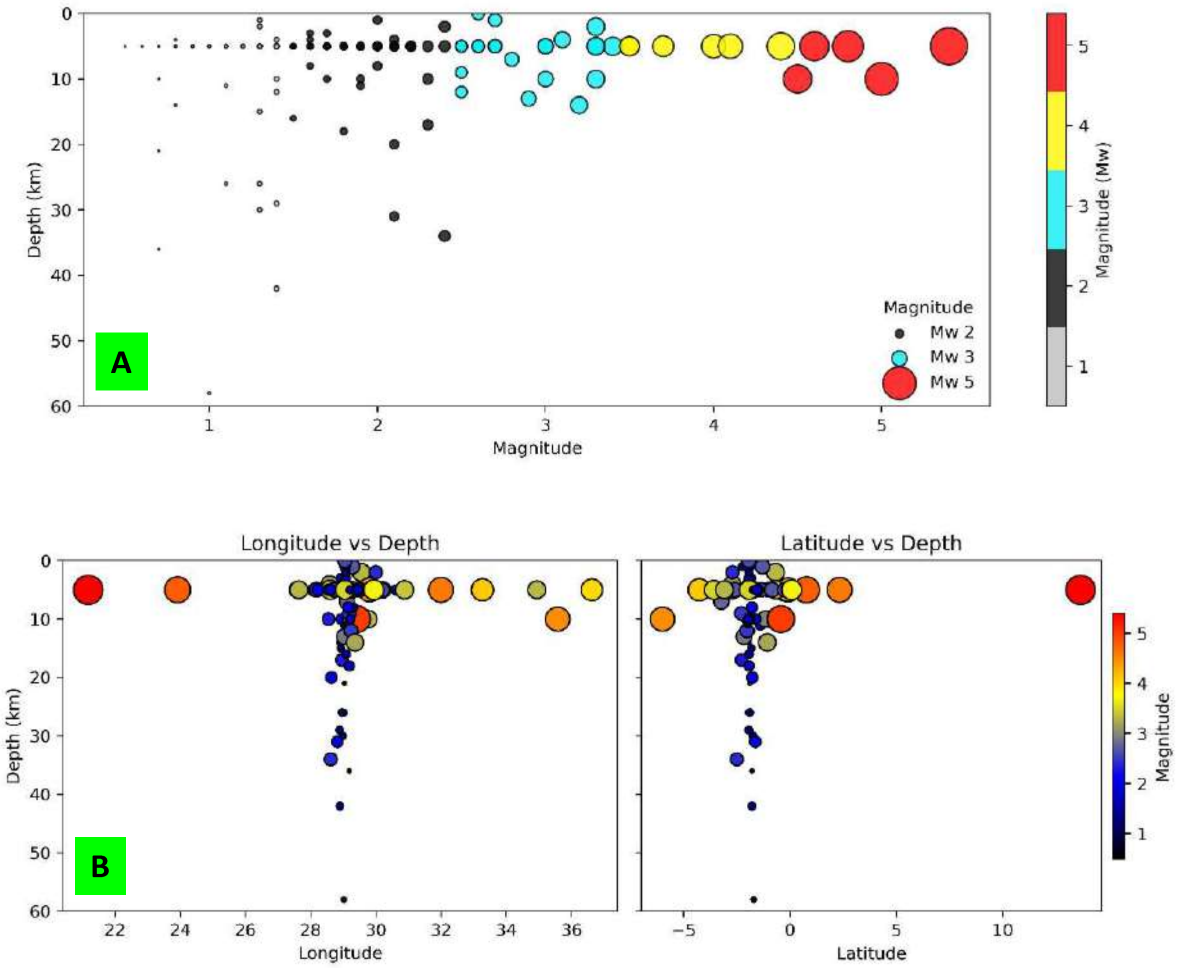

Figure 13. *(A) Earthquake magnitude vs. depth in the Virunga Volcanic Province, Western Branch of the East African Rift from April to June 2025. Circle size scales with event magnitude. Most high-magnitude events (yellow to red) are confined to <15 km depth. (B) Depth variation of earthquakes plotted against longitude (left) and latitude (right) in the Virunga Volcanic Province, Western Branch of the East African Rift from April to June 2025. Circle size scales with magnitude, and color represents magnitude using a black-to-red gradient.*

Notably, larger events tend to occur at relatively shallow depths (<15 km), which may amplify their surface impact despite moderate magnitudes. These shallow, moderate-magnitude earthquakes could pose localized hazard risks, especially near populated areas around Lake Kivu and Goma.

- **Temporal trends**

The temporal distribution of earthquakes across the three-month period (Figure 14 & 15) reveals several important trends. Seismicity occurred consistently throughout April, May, and June, with peak daily event counts exceeding 8 events/day in early April and mid-May. The cumulative event plot shows a relatively linear increase in the total number of earthquakes. This temporal persistence of low-to-moderate magnitude events indicates ongoing deformation along rift-bounding faults.

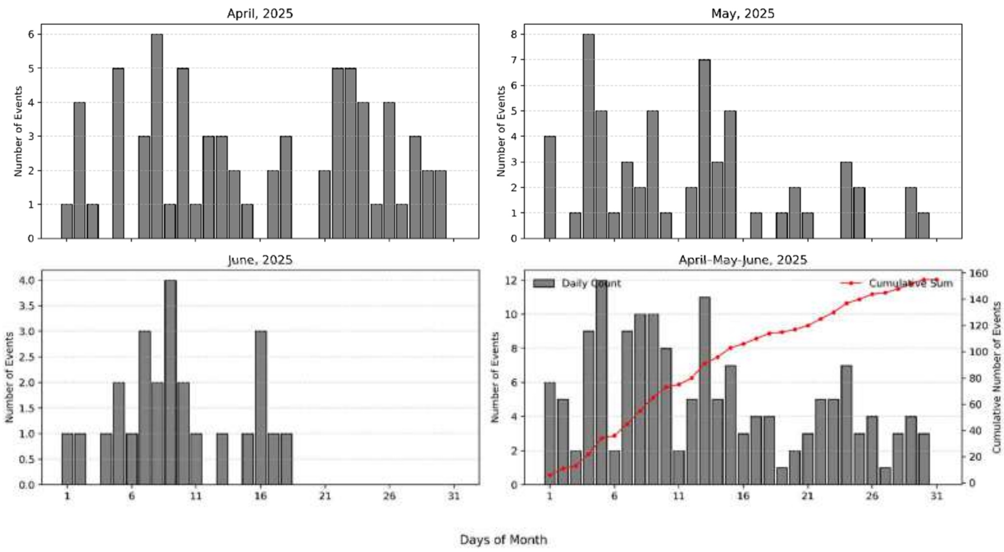

Figure 14. *Daily earthquake counts for April, May, and June 2025 (top and bottom-left panels) and cumulative count over the 3-month period (bottom-right panel, red line) in the Virunga Volcanic Province, Western Branch of the East African Rift.*

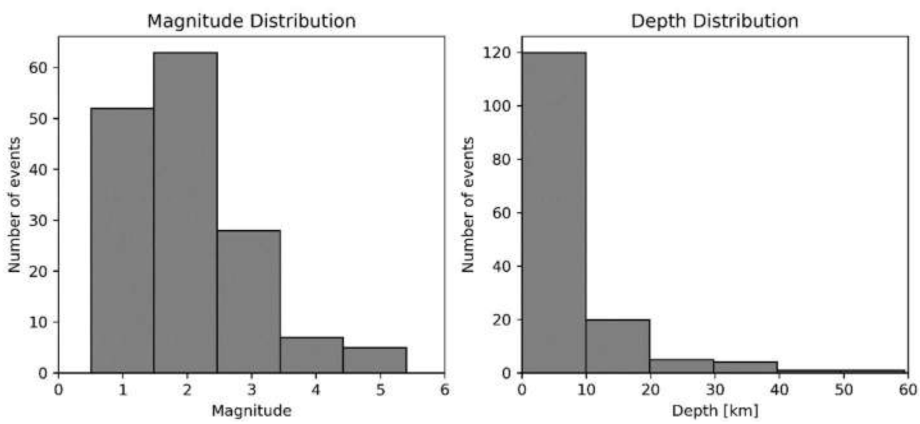

Figure 15. *Histograms showing the distribution of earthquake magnitudes (left) and focal depths (right) from April - June 2025 in the Virunga Volcanic Province, Western Branch of the East African Rift. Most events are shallow (0 - 10 km) and low magnitude (Mw 1.0 - 2.5).*

- **Seismicity concentration and hazard implications**

Kernel density estimation (KDE) results (Figure 16) illustrate zones of heightened seismicity density, with the highest concentration centered around southern Lake Kivu, near the Rwanda - DRC border. The seismicity hotspot also aligns with densely populated regions such as Goma and Bukavu, which raises concern for seismic hazard and underscores the need for real-time monitoring. Given the shallow depths and frequent low-magnitude events, even moderate earthquakes could result in damage due to local site effects and vulnerable infrastructure.

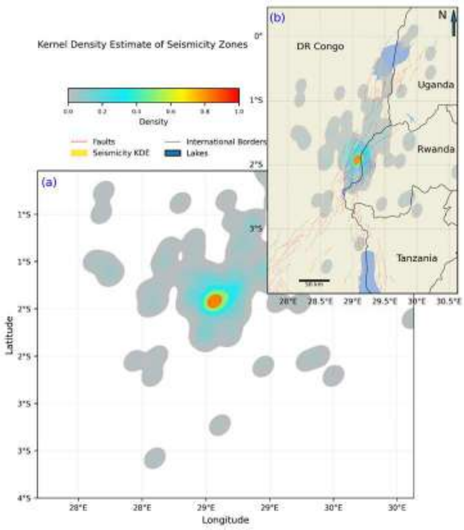

Figure 16. *(a) Kernel density estimate (KDE) map of seismicity in the Virunga Volcanic Province, Western Branch of the East African Rift from April to June 2025, normalized to maximum density. (b) Overlay of seismicity KDE on a geographic base map showing regional fault traces and tectonic boundaries in the same area during the same period as for (a).*

These findings reinforce the interpretation that both tectonic and magmatic forces contribute to seismic hazard in the Kivu Rift. The spatial correlation between seismicity, mapped faults, and volcanic features emphasizes the need for integrated geophysical and geological studies to better characterize regional risk.

- ***Conclusion***

Between April and June 2025, seismicity in the Kivu Rift region was dominated by shallow earthquakes (mostly <15 km) and low-to-moderate magnitudes (Mw 1 - 3). Events were concentrated along known rift faults, especially near Lake Kivu. Temporal patterns show steady activity with peaks in early April and mid-May, suggesting periods of increased tectonic stress.

Kernel density mapping highlights a seismic hotspot in southern Lake Kivu, aligning with active faults. These results point to ongoing crustal deformation in the Kivu Rift, driven by both tectonic extension and possible magmatic processes, underscoring the need for continued seismic monitoring in the region.

e. Seismicity patterns and tectonic context in the Virunga between July and August 2025

The seismicity recorded between June and August 2025 shows a clear concentration of earthquakes along the western branch of the East African Rift System (EARS), particularly in the Kivu Rift region (Figure 17).

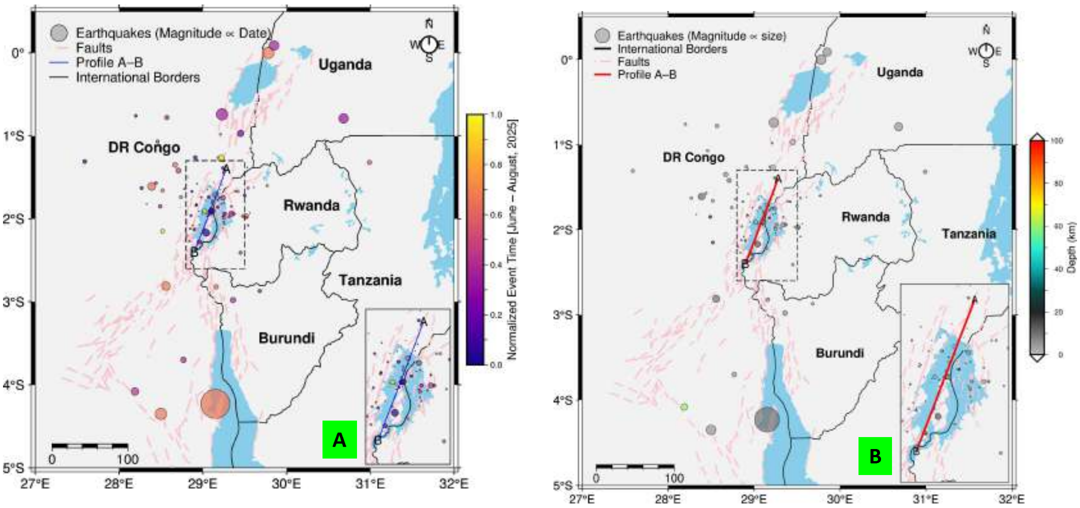

Figure 17. (A) Spatial Distribution and Temporal Evolution of Earthquakes in Virunga Volcanic Province, Western Branch of the East African Rift (June to August 2025). (B) Earthquake Depth Distribution and Magnitude in the Western Branch of the East African Rift (June to August 2025).

Depth profiles along section A–B (Figures 18) reveal that the earthquakes occur in the upper crust, mainly at depths shallower than 15 km. This pattern is typical of rift zones, where brittle failure dominates

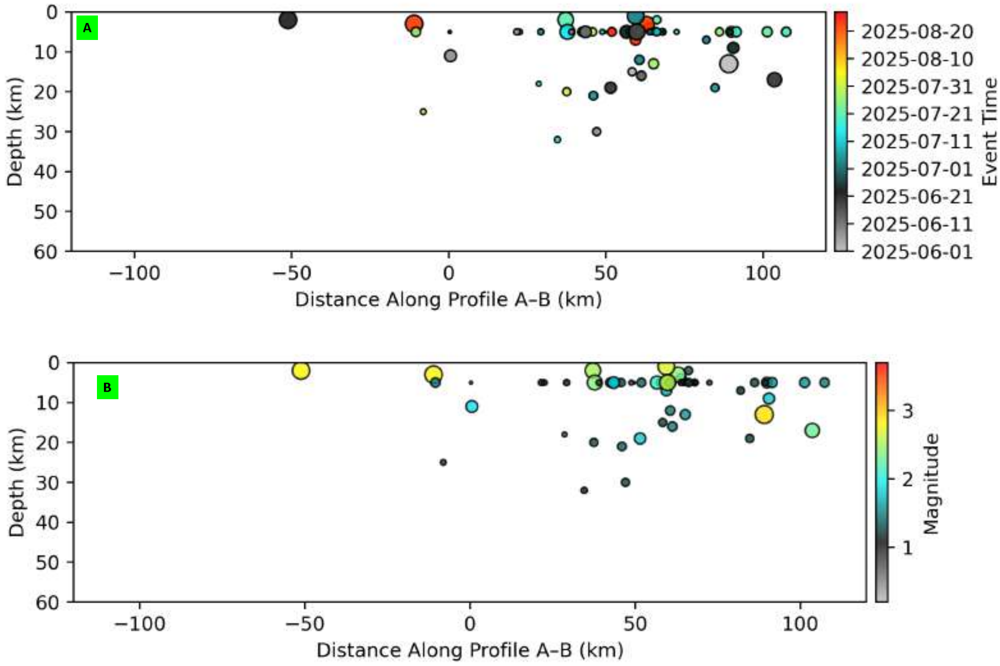

Figure 18. *Cross-Section of Earthquake Hypocenters along Profile A – B (A), (B) Spatio-temporal Distribution of Earthquake Depths along Profile A – B in Virunga Volcanic Province, Western Branch of the East African Rift from June to August 2025.*

- **Depth and magnitude characteristics**

Depth vs. magnitude analysis (Figure 19) reveals that most earthquakes occurred at shallow depths, generally less than 15 km, with few deeper than 30 km. This depth range is consistent with the brittle upper crust, where extensional faulting is most effective. The majority of events were of low-to-moderate magnitude, with a significant number clustering between Mw 1.0 and Mw 3.0, although some larger events exceeding Mw 4.5 were also recorded.

Notably, larger events tend to occur at relatively shallow depths (<10 km), which may amplify their surface impact despite moderate magnitudes. These shallow, moderate-magnitude earthquakes could pose localized hazard risks, especially near populated areas around Lake Kivu and Goma.

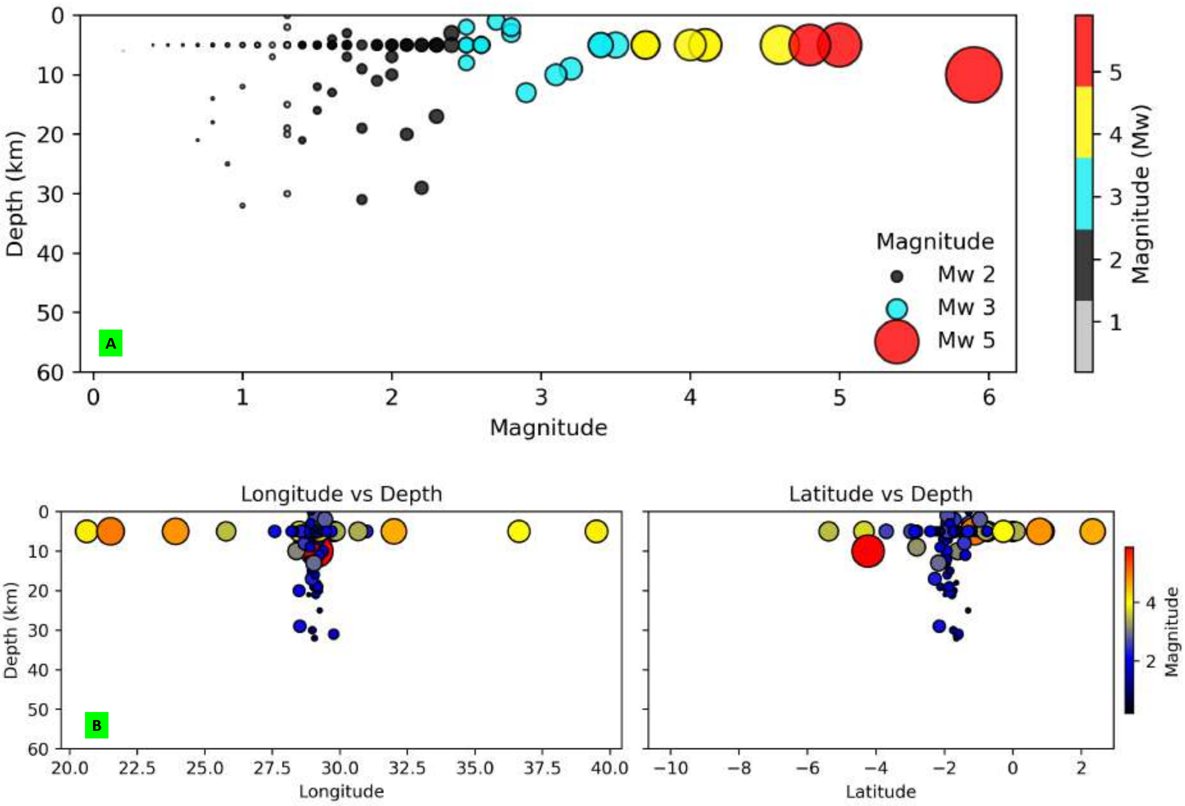

Figure 19*. (A) Earthquake magnitude vs. depth in the Virunga Volcanic Province, Western Branch of the East African Rift from June to August 2025. Circle size scales with event magnitude. Most high-magnitude events (yellow to red) are confined to <15 km depth. (B) Depth variation of earthquakes plotted against longitude (left) and latitude (right). Circle size scales with magnitude, and color represents magnitude using a black-to-red gradient.*

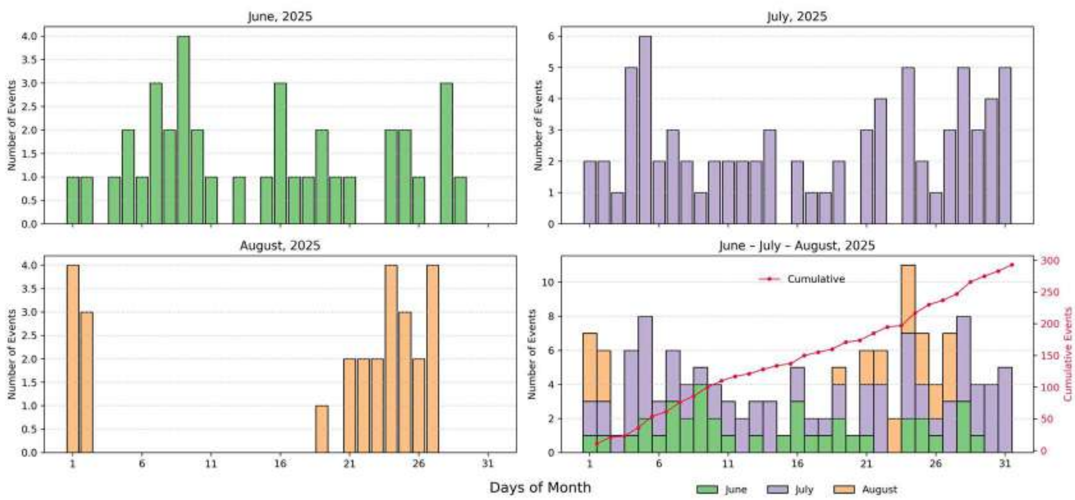

Figure 20. *Daily earthquake counts for June, July and August 2025 (top and bottom-left panels) and cumulative count over the 3-month period (bottom-right panel, red line) in the Virunga Volcanic Province, Western Branch of the East African Rift System.*

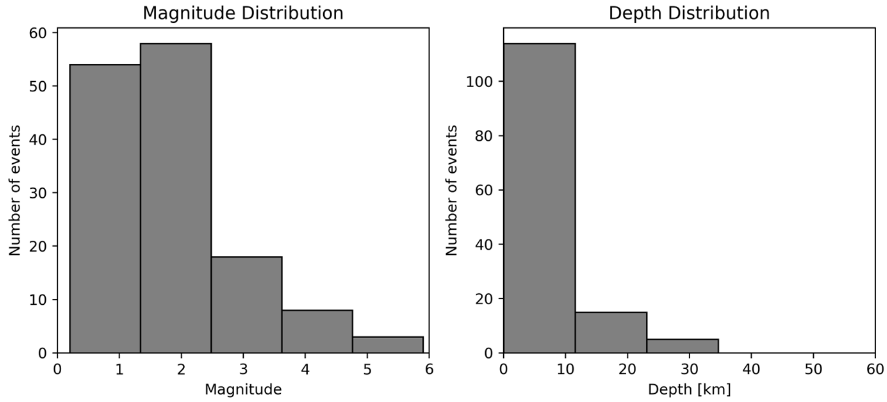

Figure 21. *Histograms showing the distribution of earthquake magnitudes (left) and focal depths (right) from June to August, 2025 in the Virunga Volcanic Province, Western Branch of the East African Rift System. Most events are shallow (0 - 10 km) and low magnitude (Mw 1.0 – 3.0).*

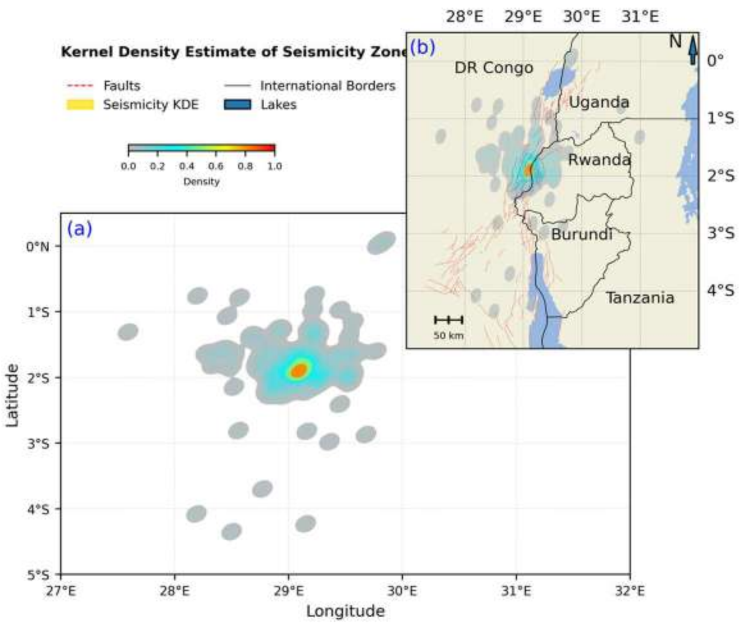

*Figure 22. **(a)** kernel density estimate (kde) map of seismicity from June to august 2025 the Virunga Volcanic Province, Western Branch of the East African Rift System, normalized to maximum density. **(b)** overlay of seismicity kde on a geographic base map showing regional fault traces and international borders.*

- **Seismicity concentration and hazard implications**

Kernel density estimation (KDE) results (Figure 22) illustrate zones of heightened seismicity density, with the highest concentration centered around southern Lake Kivu, near the Rwanda - DRC border. The seismicity hotspot also aligns with densely populated regions such as Goma and Bukavu, which raises concern for seismic hazard and underscores the need for real-time monitoring. Given the shallow depths and frequent low-magnitude events, even moderate earthquakes could result in damage due to local site effects and vulnerable infrastructure.

These findings reinforce the interpretation that both tectonic and magmatic forces contribute to seismic hazard in the Kivu Rift. The spatial correlation between seismicity, mapped faults, and volcanic features emphasizes the need for integrated geophysical and geological studies to better characterize regional risk.

Conclusion

Between June and August 2025, seismicity in the Kivu Rift region was dominated by shallow earthquakes (mostly <10 km) and low-to-moderate magnitudes (Mw 1 – 3.5). Events were concentrated along known rift faults, especially near the lake. Kernel density mapping highlights a seismic hotspot in southern Lake Kivu, aligning with active faults. These results point to ongoing crustal deformation in the Kivu Rift, driven by both tectonic extension and possible magmatic processes, underscoring the need for continued seismic monitoring in the region.

5.1.2. Volcanic gases measurement and associated hazards assessment

Measuring volcanic gases is critically important at Nyiragongo and Nyamulagira volcanoes because degassing at these two highly active basaltic systems provides direct, near–real-time information on magma dynamics occurring at depth. Among all monitoring parameters used by the OVG, volcanic gas emissions are among sensitive indicators of magma movement, conduit processes, and changes in eruptive behavior (e.g. Balagizi et al., 2016; Bobrowski et al., 2017).

At Nyiragongo and Nyamulagira, variations in gas composition and flux are routinely used for eruption forecasting and early warning. As magma ascends and depressurizes beneath these volcanoes, changes in gas output signal magma intrusion, conduit opening, or sealing processes. For example, increases in CO_2 emissions, which exsolve at greater depths than SO_2, often precede eruptive episodes and can indicate deep magma recharge within the plumbing systems of both volcanoes. In contrast, elevated SO_2 fluxes are commonly associated with shallow magma ascent and active lava effusion, particularly at Nyamulagira.

Continuous and periodic gas monitoring using DOAS stations, MultiGAS, and portable gas analyzers therefore represents a key tool for short- to medium-term eruption forecasting at these volcanoes (e.g. Arellano et al., 2017; Balagizi et al., 2023, 2016). Such measurements are essential for identifying zones of elevated volcanic gas concentrations that pose direct hazards to nearby populations, especially in Goma and surrounding communities, and for supporting land-use planning, civil protection strategies, and emergency response (Balagizi et al., 2018).

Finally, gas emissions from Nyiragongo and Nyamulagira have significant environmental and climatic impacts (Balagizi et al., 2017; Cuoco et al., 2013b, 2013a; Kasereka et al., 2017, 2021). Large releases of SO_2 and CO_2 influence atmospheric chemistry, air quality, and acid deposition, while gas–water interactions can alter surface and groundwater chemistry in the region (Balagizi, 2016; Balagizi et al., 2015, 2017; C. M. Balagizi et al., 2022). Consequently, sustained volcanic gas monitoring (Figure 23) is essential not only for hazard mitigation but also for understanding the broader environmental impacts of these two major African volcanoes.

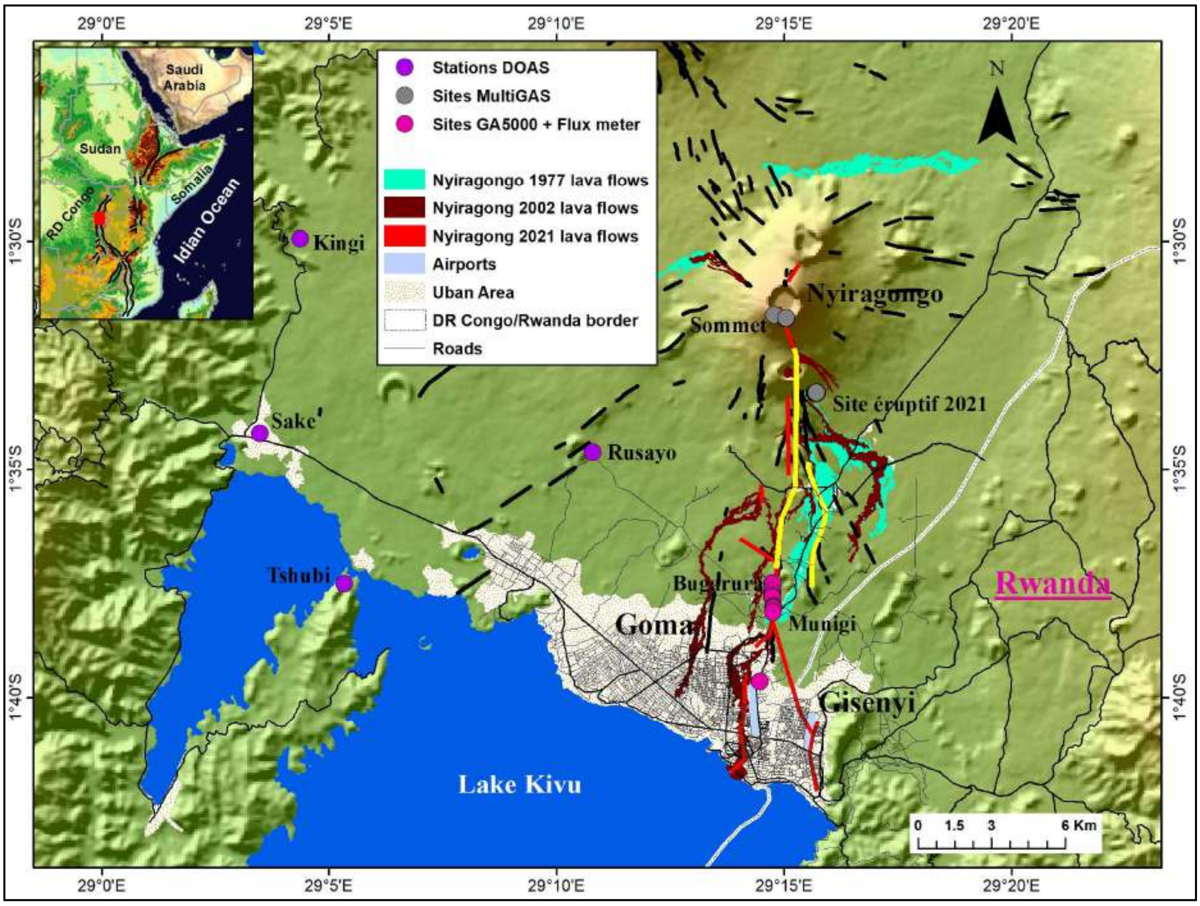

***Figure 23**. Map showing the sites where gases are measured around Nyiragongo and Nyamulagira volcanoes in the Virunga Volcanic Province, East African Rift System. DOAS stations are permanently installed in the field, the other measurements are made twice a week during field campaigns.*

5.1.2.1. Sulphur dioxide emitted by Nyiragongo Volcano by DOAS

Gas emissions from the crater of Nyiragongo volcano completely disappeared immediately after the May 2021 eruption, following the drainage of its lava lake during the eruptive event. However, within a few months after the eruption, effusive activity resumed inside Nyiragongo crater, leading to a gradual reappearance of the volcanic gas plume and later on its persistent visibility from Goma city. Consequently, during the year 2024 the SO_2 fluxes had already reached significant levels. These flux values, calculated from data acquired at the Rusayo station, indicate that Nyiragongo volcano has developed appreciable and continuous degassing activity. Despite some data gaps caused by power supply failures at the station, the measurements provide a reliable indication of the general trend and intensity of gas emissions (Figure 24).

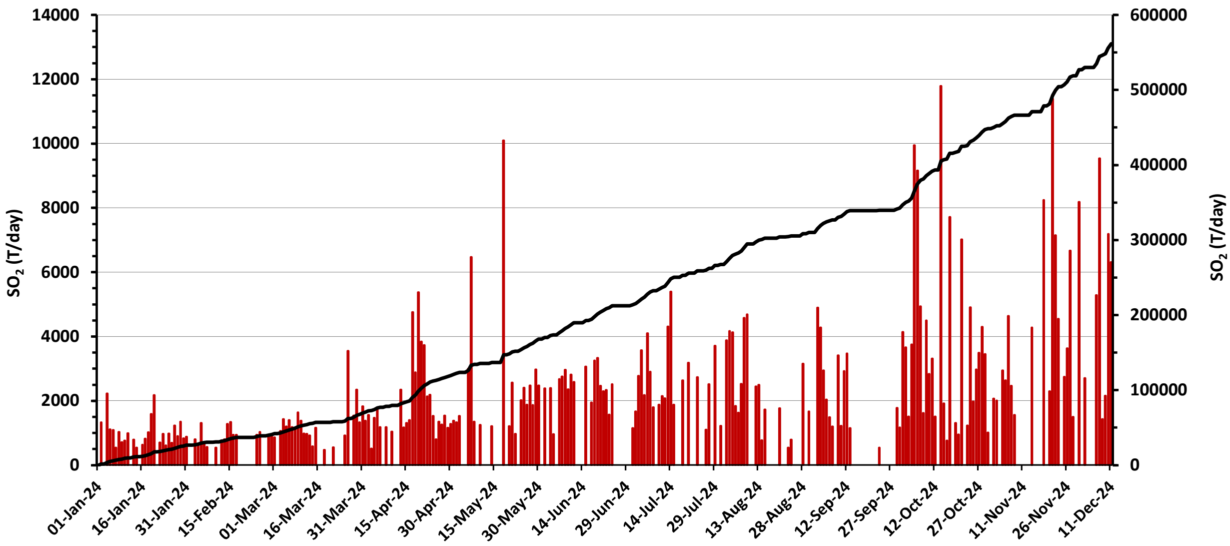

Figure 24. Variation of SO_2 fluxes from Nyiragongo volcanic plume as measured at Rusayo site between January and December 2024, in the Virunga Volcanic Province.

This figure shows that from April 2024 onward, consistently high SO_2 flux values were obtained. Several pronounced peaks were recorded, reaching 11,785.98 tons per day on 14 October 2024 and 11,395.14 tons per day on 21 November 2024. This pattern reflects a period of intense and sustained degassing activity within the Nyiragongo crater. It is noteworthy that such high SO_2 flux values had not been recorded in the Nyiragongo plume for several years. Unfortunately, the Rusayo DOAS station, which was the only remaining operational station, was vandalized during the conflict in late January 2025. As a result, continuous SO_2 measurements are no longer being carried out.

5.1.2.2. CO_2 hazards assessment in war displaced persons camps

Mazuku, a term meaning devilish wind or evil places, are CO_2-rich and oxygen-depleted zones within the Virunga Volcanic Province where humans and animals can die from asphyxiation. They are typically dry gas vents located in topographic depressions or along lava flow fronts, where volcanic CO_2 ascends to the surface and accumulates because it is denser than air. CO_2 concentrations in mazuku are generally low during the day but can rise to lethal levels at night, early morning, evening, or after rainfall, particularly under low temperature and wind conditions. Acting as natural traps, they may sequentially attract insects, predators, and eventually humans, with children being especially vulnerable due to their height and daily activities such as firewood collection. High CO_2 effects are often culturally interpreted as supernatural phenomena (read more in Balagizi et al., 2018; Kasereka et al., 2017; Vaselli et al., 2003).

Figure 25. Map showing the location of mazuku and war displaced persons camps in the north catchment of Lake Kivu, where concentrations range from 20 to 71% depending on location in June 2013 (left, after Balagizi et al., 2018). CO_2 concentration measurements in war displaced persons camps in May 2024 using a MultiGAS instrument (right).

Unfortunately, it is in these hazardous places where war displaced camps are established (Figure 25, left) during local and regional political unrest which were recurrent over the last 30 years.

Numerous fatalities have been recorded in the war displacement camps, predominantly among displaced persons collecting firewood or performing other similar activities within or around the camps—areas where mazuku (CO_2 gas emission zones) are also present. In response to this hazard, GVO teams have contributed to mitigating this risk through the reduction of the exposure by conducting measurement campaigns to assess CO_2 concentrations within the camps (Figure 25, right) and by installing warning signs to indicate the presence of mazuku zones (Figure 26).

Figure 26. Some warning signs to indicate the presence of mazuku zones near war displaced camps near Goma city in June 2024.

An example of the CO_2 concentrations in the Rego/CEBCA sector of the series of camps is given in the following observations were noted with the measurement results shown in Figure 27.

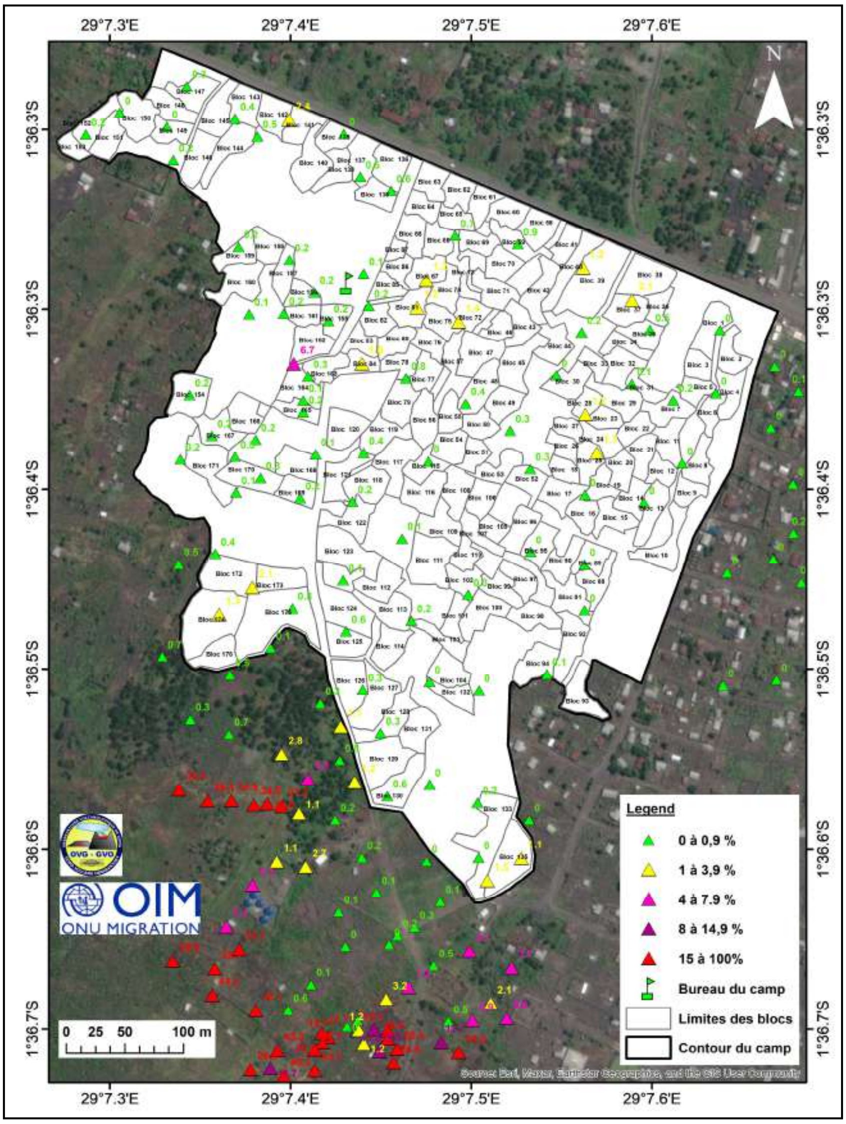

Figure 27. Map of the Rego/CEBCA site showing the locations where measurements were carried out (within the camp and its immediate surroundings) in May 2024.

- Most of the place with tents are located (see block locations) present no risk, as the CO_2 concentrations are below 1%. Some points show concentrations between 1 and 3.9%, values that remain below the acceptable exposure limit.
- Between blocks 162, 163, and 164 (Figure 27), one point shows concentration of 6.7%.
- To the south and southwest, outside the camp but within its immediate surroundings, there are very high-risk zones with CO_2 concentrations above 15%, and even exceeding 40%.

5.1.3. *Geochemistry: Lake Kivu*

Between April and September 2025, a series of systematic water sampling campaigns were carried out on Lake Kivu and in groundwater located in Goma city. The additional sampling efforts of groundwater from wells were designed to provide the information about the quality of water resources that are essential for the local population. Lake Kivu, being a transboundary lake situated in the western branch of the East African Rift, plays a vital role not only as a natural reservoir but also as a source of water for domestic use, fisheries, and ecological balance. In parallel, the groundwater wells scattered across Goma city serve as an important source of drinking water for many households, especially in areas where piped water supply is limited or irregular.

The field campaigns consisted of collecting water profiles along the water column of the lake, complemented by well-water sampling from different neighborhoods in Goma. The sampling design allowed comparison between surface water and groundwater systems, which are both heavily influenced by regional geological and volcanic settings. Some of the collected samples were kindly analyzed by the Rwanda Environment Management Authority (REMA) team, and the results were shared in a timely manner. This collaboration proved particularly valuable because the data provided direct support for water quality demands from users, particularly concerning well-water safety for human consumption.

Several key parameters were systematically measured during these campaigns. Physical and chemical variables, including water temperature, specific conductivity, pH, and dissolved oxygen (DO), were monitored (Figures 28, 29 and 30). These indicators are fundamental for understanding the hydro chemical state of the water and for detecting potential anomalies that may signal contamination or unusual geochemical processes. Temperature and DO profiles, for instance, are crucial in assessing the stratification of the lake, which is known to harbor large amounts of dissolved gases such as methane and carbon dioxide at depth. Conductivity values, on the other hand, provide information about the concentration of dissolved ions, which may originate from natural geochemical processes, volcanic inputs, or anthropogenic pollution.

In addition to these parameters, biological and optical measurements were performed. Chlorophyll-a concentration was recorded as a proxy for phytoplankton biomass and primary productivity in the lake. This information is important for assessing ecological health and nutrient dynamics, since excessive algal growth can compromise water quality and affect aquatic biodiversity. Turbidity, another measured parameter, served to evaluate water clarity and the presence of suspended particles. Turbidity values are influenced by runoff, sediment input, or organic matter, and can have direct implications for drinking water quality and ecosystem functioning.

All measurements were conducted using a CTD (Conductivity-Temperature-Depth) probe, which allowed high-resolution vertical profiling of the lake waters and rapid in-situ monitoring of the wells. This modern instrument ensured accurate data acquisition, which was then processed and interpreted in the framework of the ongoing project. The results obtained provide a valuable baseline for understanding both the natural variability of Lake Kivu's limnology and the potential risks faced by groundwater resources in the city.

Figures accompanying this report illustrate some of the datasets obtained during the different field campaigns. They highlight variations between sampling stations, potential seasonal changes, and differences between lake and well waters. Overall, these results contribute significantly to advancing knowledge on water geochemical composition and quality in a region where both volcanic activity and human pressures strongly shape the hydro-environmental system.

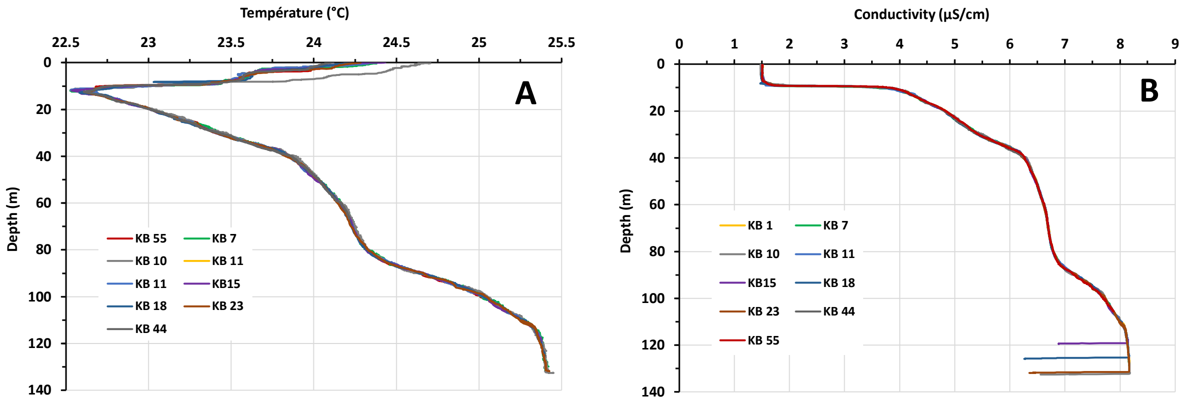

Figure 28. Temperature (A) and conductivity (B) variations along the water column of Kabuno Bay, a sub basin of lake Kivu as measured between April and September 2025**.**

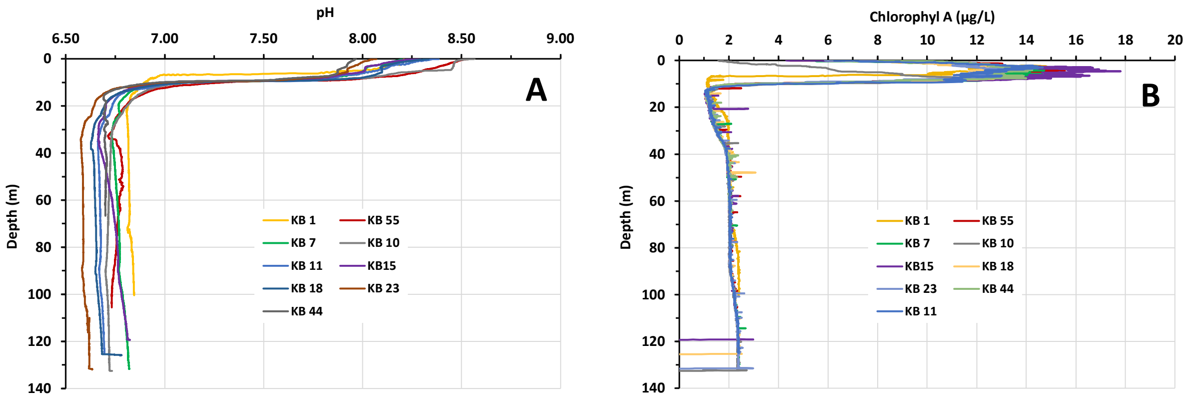

Figure 29. pH (A) and chlorophyl A (B) variations along the water column of Kabuno Bay, a sub basin of lake Kivu as measured between April and September 2025.

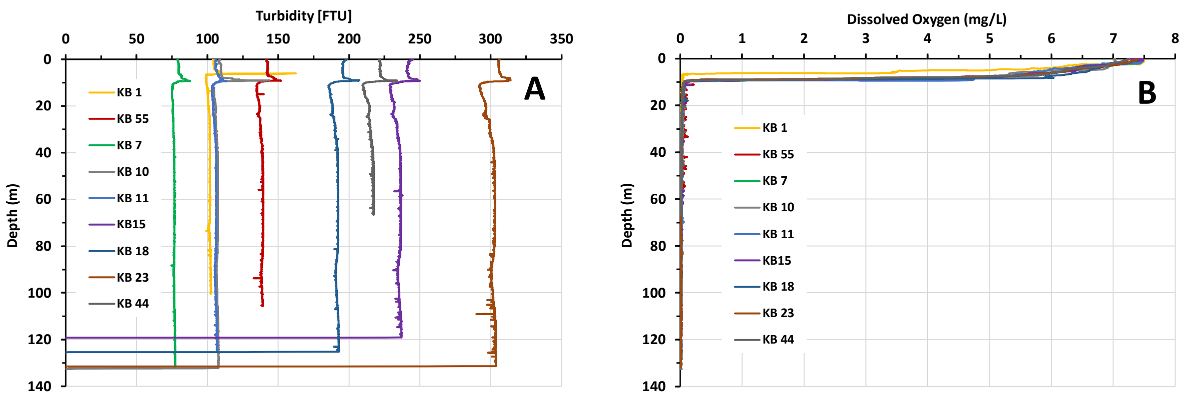

Figure 30. Turbidity (A) and dissolved oxygen (B) variations along the water column of Kabuno Bay, a sub basin of lake Kivu as measured between April and September 2025.

As part of the sampling campaign, several physico-chemical parameters were analyzed. The results, summarized in Table 1, reveal significant variability of the values between the different lake sites. The average surface water temperature ranges between 21.20 °C and 25.79 °C depending on the sampling sites. This variation is mainly attributed to the density of riparian vegetation as well as the time of sample collection. The average dissolved oxygen (DO) content varies between 6.57 mg/L and 8.36 mg/L. This variability is strongly correlated with temperature: an increase in temperature tends to raise dissolved oxygen concentration, while a decrease leads to a reduction. The pH remains basic across all sites, with average values ranging from 7.73 to 9.63. This variation is influenced by ion concentration, the nature of the geological substrate, as well as human activities carried out near the sampling points.

5.2. Satellite Data

5.2.1. Nyamulagira volcano activity monitored by SAR interferometric coherence

From July 2023 Nyamulagira volcano has been showing a marked increase in activity, including effusive eruptions, seismicity, gas and ash emissions, and thermal anomalies. After its last flank eruption that occurred from 6 November 2011 to mid-April 2012 (Balagizi et al., 2016, 2018b; Coppola et al., 2016a), activity mainly concentrated inside the northeastern pit crater, where intermittent lava-lake conditions have been reported over the last decade (Burgi et al., 2021). Based on GVO weekly reports and satellite monitoring (MIROVA and MOUNTS) (Coppola et al., 2016b; Valade et al., 2019). The overall threats posed by Nyamulagira volcano are both environmental and socioeconomic, with the potential to displace communities, disrupt ecosystems, and damage livelihoods and infrastructures such as agricultural service roads. Nyamulagira lava flows do not directly threaten Goma city because Nyiragongo prevents lava from Nyamulagira reaching Goma, however the lavas have reached and destroyed small cities and villages to its south (Figure 31). As an open system volcano, Nyamulagira continuously releases acidic gases (e.g. CO_2, SO_2, HCl, HF) and ash to the atmosphere of which the amounts increase during effusive flank eruptions, these gasses and ash yield air pollution, cause respiratory problems, and lead to acid rain and high fluoride content in surface water which affect both the environment and human health (Balagizi et al., 2015, 2017, 2018a; C. M. Balagizi et al., 2022; Cuoco et al., 2013b, 2013a; Kasereka et al., 2021). The worst-case scenario of an eruption of Nyamulagira volcano would occur to its southern flanks and produce lava flows that would potentially destroy small cities such as Sake, Mubambiro, Nzulo, Bulengo (similar to the 1938, 1948 or 1986 eruptions, Figure 31) and the displaced refugee camps which are all located to the south of the volcano. The lava flows could also damage the Goma-Sake Road and deprive Goma of fresh food and other supplies, or even reach Kabuno Bay in sufficient volumes, rate and heat, they could cause a limnic eruption of the bay, releasing dissolved gasses from the lake (Balagizi et al., 2018b). Hence, there is a strong need for improving the study and monitoring of Nyamulagira so that early warnings can be given to protect the communities living in cities and villages located to the south of the volcano from potential dangers, such as lava flows, toxic gas emissions and ash and to continuously be aware an eruption could potentially yield a lake Kivu overturn.

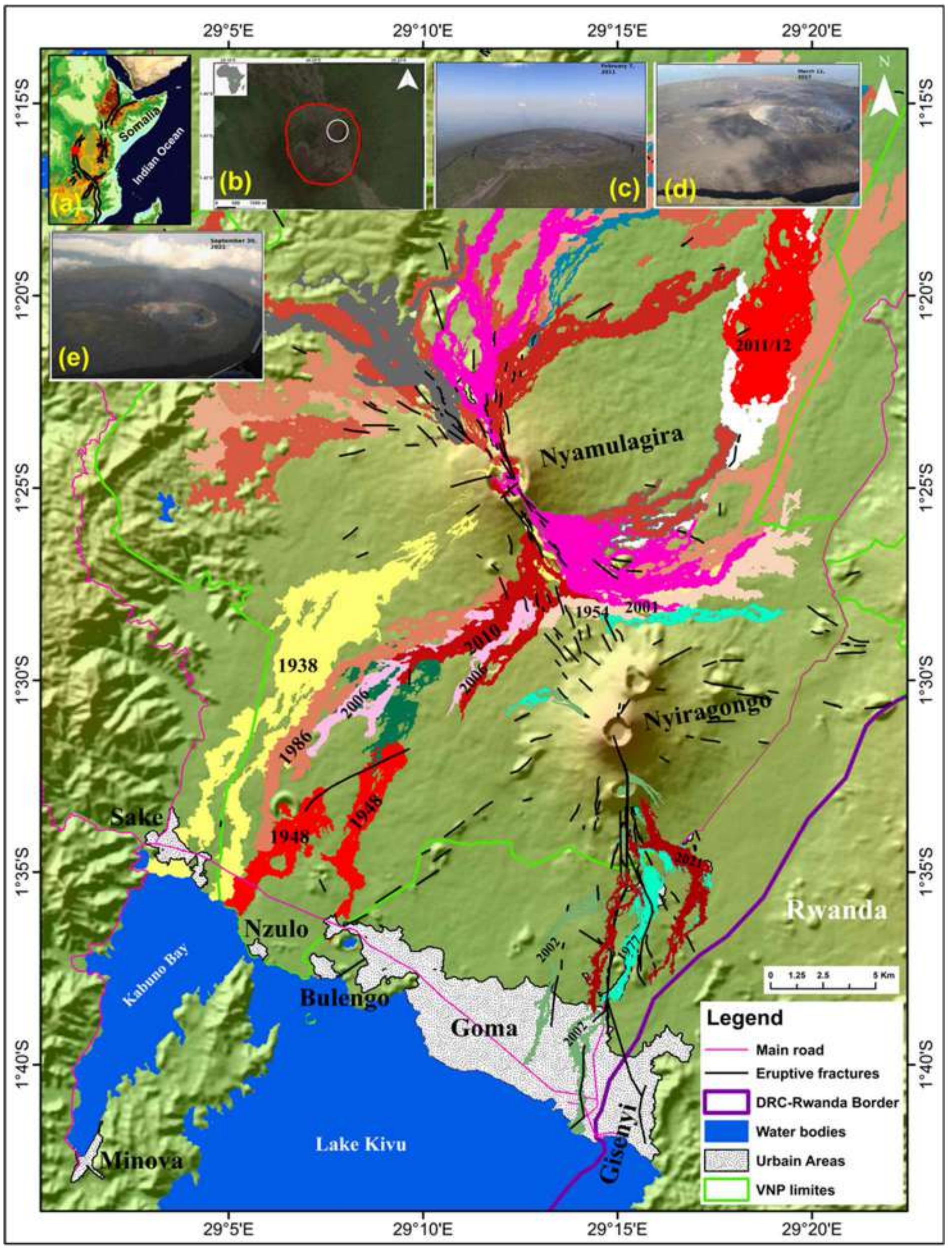

Figure 31. Map showing the recent lava flows of Nyamulagira and Nyiragongo and inhabited areas located to the south of the two volcanoes, as well as the historical lava flows of Nyamulagira that have reached cities and villages (Modified from *Balagizi et al., 2018)*. The inset map (a) shows the location of the Virunga volcanic province in the East African Rift, while the panels (b) focus respectively on the Nyamulagira volcano on Esri satellite where the red and the white polygons indicate the caldera and the NE crater pit, (c) the aerial photo of the crater on February 7, 2011, (d) on March 11, 2017, and (e) on September 30, 2021. Old overflows are visible on panels (b) and (c).

Field monitoring of Nyiragongo and Nyamulagira volcanoes is hampered by insecurity and armed groups (Balagizi et al., 2020, 2018b; Balagizi et al., 2022; Sadiki et al., 2023), increasing the value of SAR remote sensing. Multi-temporal InSAR coherence was exploited to analyze several phenomena during Nyamulagira volcano activity, a significant increasing of the activity was observed with several eruptions and a lava lake inside the northeastern crater pit. SAR data were exploited to follow the temporal evolution of the volcanic activity by the analysis of any InSAR coherence variations. The aim is to detect any lava flows inside the caldera and overflowing the flanks of the volcano. In addition, the time needed for the lava to solidify is tentatively estimated by studying the statistical behavior of the coherence pattern ascribable to a lava flow. Experimental results show a significant lava effusion inside Nyamulagira caldera from the beginning of March, while in mid-May the increase of the activity induced an overflowing from the caldera with a lava flow observed along the NW flank of the volcano. Then, starting from the end of May-early June, the activity started to return to low levels. The statistical analysis of the probability distributions suggests that after the crisis of May, the lava follows a solidification and likely cooling phase with an approximate time to complete the process estimated in 45/50 days. These results were synergistically used with other data to support the GVO local monitoring team in managing the May 2023 Nyamulagira volcano crisis.

A. Data

The SAR dataset used consists of 27 and 31 images acquired by Sentinel-1 missions of ESA along ascending and descending satellite track. The geometry of view is characterized by an incidence angle of about 34◦ (ascending) and 39◦ (descending) and an azimuth angle of about 12◦. The images were multi-looked by 4x1 factor along range and azimuth to get square pixels of the output products of about 15m. The Digital Elevation Model (DEM) exploited in the InSAR processing steps and for geocoding the products is the one acquired by the Shuttle Radar Topography Mission (SRTM) with a resolution of about 30 m. In addition, a pair of Cosmo-SkyMed- Second Generation (CSG) data was used in the validation step. These images were acquired in Stripmap mode and along ascending track. The incidence angle of the acquisitions is about 32◦ whereas the azimuth angle is about 11◦. They were processed at full resolution with a pixel spacing of about 3 × 3 m and also in this case the 30 m SRTM DEM was used for geocoding the retrieved products.

B. Caldera monitoring

The first outcome retrieved for this analysis is the time series of the mean coherence estimated, for each coherence map, by averaging all the coherence pixel values inside the caldera ash shown below in figure 32.

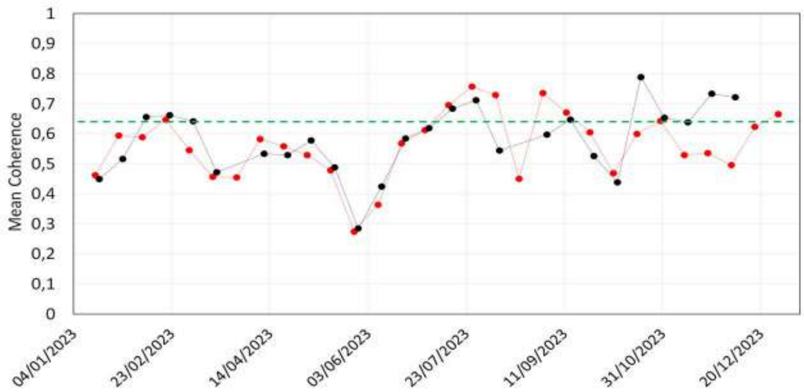

Figure 32. Nyamulagira time series of mean coherence estimated with Sentinel ascending (red) and descending (black) from January to December 2023. The green dashed line indicated the coherence reference estimated during the low activity period**.**

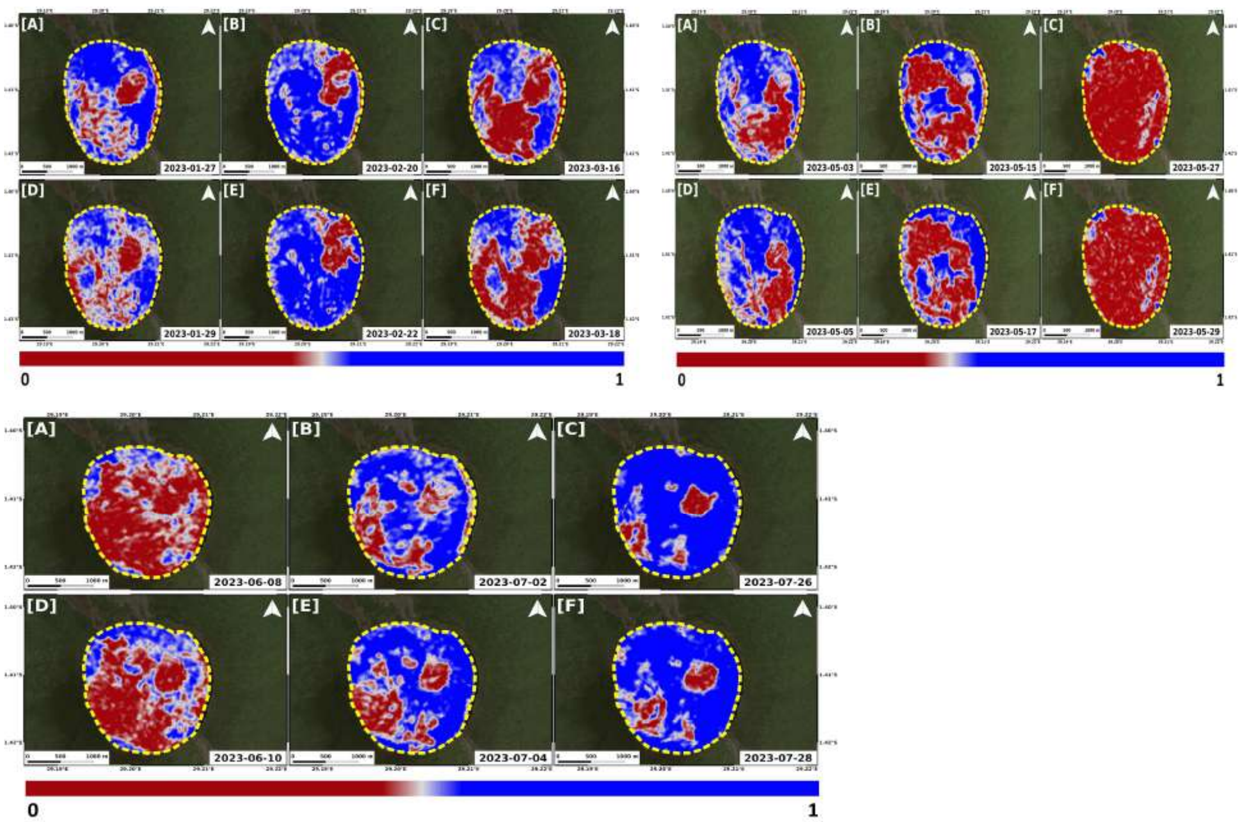

Figure 33. Nyamulagira coherence maps cropped in correspondence with the caldera estimated before and after the crisis of May 2023 along ascending (A, B, C) and descending (D, E, F) track using Sentinel data

C. Lava Flows detection

The following analysis aims to detect any lava flows overflowing the caldera along the flanks of Nyamulagira volcano. The results are shown in Figure 34. A clear lava flow is detected along the NW flank of the volcanic building mainly westward/south-westward moving and an additional small lava flow is observed less than 1 Km north. The main lava flow covers an area of approximately 1.8 Km^2 with some ramifications reaching a distance from the caldera of about 2.5 Km.

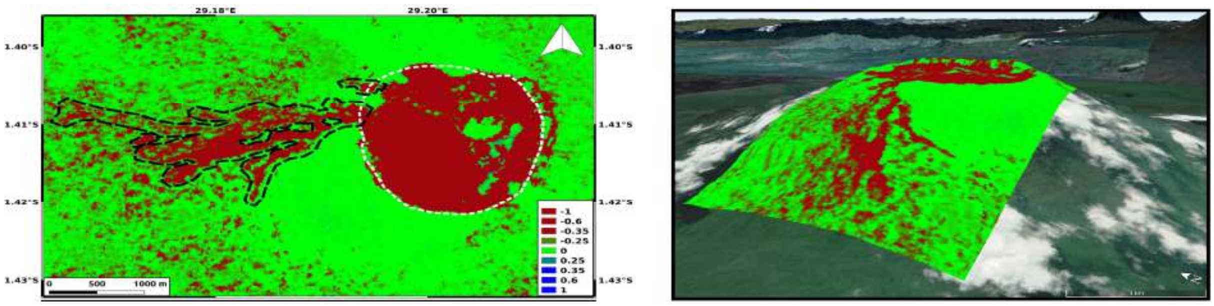

Figure 34. Nyamulagira coherence map estimated by averaging ascending and descending coherence maps of May 15th-27th and 17th-29th 2023, respectively (left panel). The dashed white polygon indicates the caldera of Nyamulagira whereas the dashed black polygons represent the lava flows detected with this analysis from Sentinel data.

D. Lava solidification time

By examining coherence histograms of the NW flank, the authors modelled transitions from Lognormal (eruptive) to Normal (cooling) and Left-Skewed Gumbel (solidified) distributions. The coherence mode rose from 0.22 in May to 0.8 by mid-July 2023, indicating a solidification period of ~45–50 days. This result, if validated in other contexts, could serve as a proxy for estimating lava cooling durations in future eruptions (Figure 35).

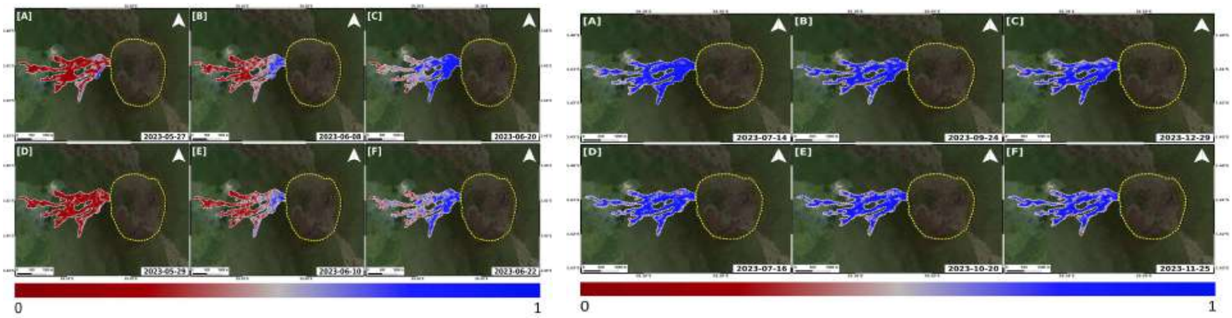

Figure 35. Coherence maps cropped in correspondence with the NW lava flow during and just after the crisis of May along the ascending (A, B, C) and descending (D, E, F) track of Sentinel in May 2023.

5.2.2. Assessing potential ground deformation over Virunga volcanoes caused by the May-June 2024 effusive activity of the Nyamulagira volcano

1. Introduction

Following the June 2024 Virunga Supersite coordinator's request to monitor an anomalous effusive activity of the Nyiragongo volcano lava lake, the INGV GEOSAR Laboratory processed both C-band Sentinel-1 and L-band SAOCOM SAR data. With the aim of detecting possible volcano-induced deformation, several ascending interferometric pairs were initially considered starting from January 2024. However, despite different spatial and temporal baselines being explored, no clear deformation patterns were identified. The area is challenging to be studied with SAR data because of the complex topography, the strong atmospheric artefacts and the vegetation cover, which cause temporal decorrelation effects. Moreover, the most recent SAR acquisitions were characterised by long spatial baselines, producing spatial decorrelation effects, especially for the SAOCOM data.

Thus, in order to try mitigating such effects, a multi-temporal analysis was performed considering Sentinel-1 acquisitions from January 2023 to the end of June 2024, employing both ascending and descending orbit data. Nyiragongo volcano and Goma city were analysed through the Small BAseline Subset (SBAS) technique. Considering its recent activity, a further analysis was performed at Nyamuragira volcano using the Interferometric Point Target Analysis (IPTA) technique. No multi-temporal analysis was performed using SAOCOM data because of the limited number of available images.

2. Data and Methods

The Nyiragongo volcano deformation was monitored using Sentinel-1 ascending and descending orbits. The applied multi-temporal algorithm was the SBAS (Lanari et al., 2004) as implemented in the Sarscape software. The area of interest considered for the SBAS is shown in Figure 36.

The Nyamuragira volcano deformation was investigated using Sentinel-1 ascending orbit data using the IPTA approach (Wegmuller and Werner, 1997) implemented in the GAMMA software. The processed area is shown in Figure 36.

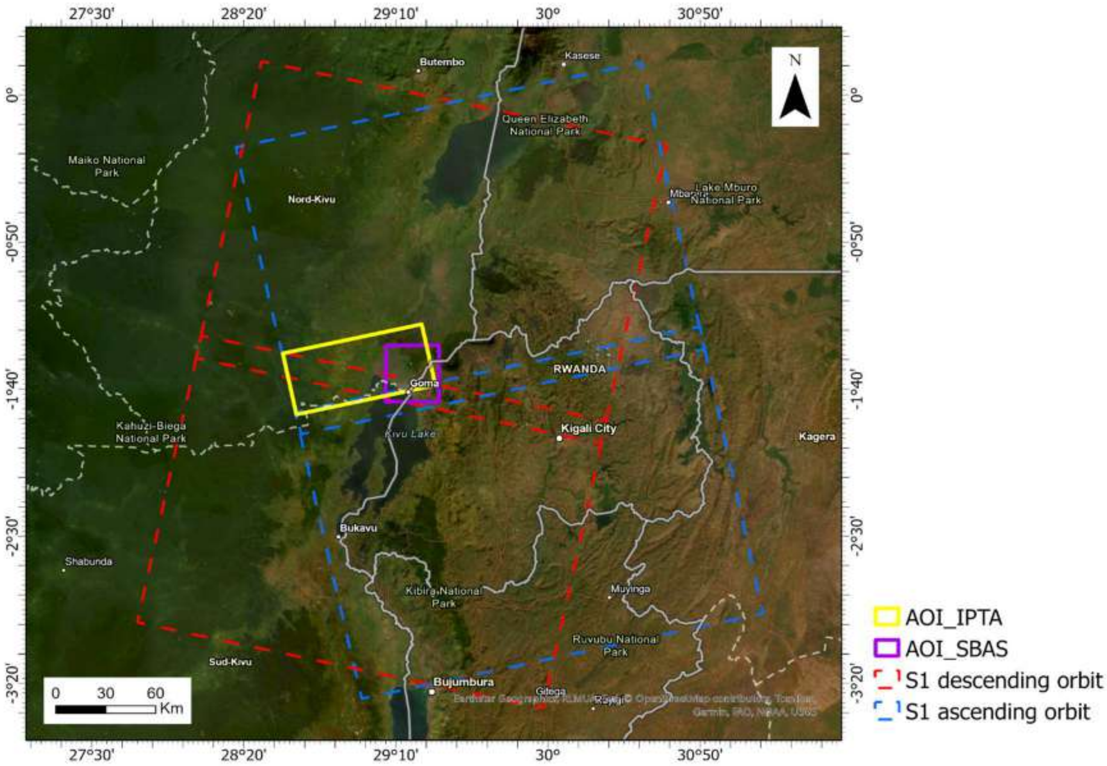

Figure 36. Overview of the study area. Light blue and red dashed polygons identify Sentinel-1 ascending and descending orbits, respectively. Yellow and purple polygons show areas processed through IPTA and SBAS algorithms, respectively.

The characteristics of the Sentinel-1 datasets used for each technique are reported in Table 1.

Table 1. Characteristics of the processed Sentinel-1 datasets

	SBAS		IPTA
Orbit	Ascending	Descending	Ascending
Track number	174	21	174
No. of images	45	42	42
Data Product	Level 1 - Single Look Complex (SLC)	Level 1 - Single Look Complex (SLC)	Level 1 - Single Look Complex (SLC)
Acquisition Mode	Interferometric Wide (IW) Swath	Interferometric Wide (IW) Swath	Interferometric Wide (IW) Swath
Start Date	20230103	20230105	20230103
End Date	20240626	20240616	20240626
Revisit Time	12 days	12 days	12 days

3. Results

3.1. Nyiragongo volcano and Goma city

The ascending deformation rate map derived by the SBAS algorithm highlights a constant negative trend inside the Nyiragongo crater with velocities <-10 mm/yr (Figure 37a). Along the descending orbit, the deformation rate map shows a general negative trend inside the crater with velocities of <-2 mm/yr (Figure 37b).

The ascending ground displacement time series for the area of the crater reveal a trend variation starting from the end of 2023. The descending time series identified no particular trend variation before and during the unrest period of the volcano (Figure 37c,d&e).

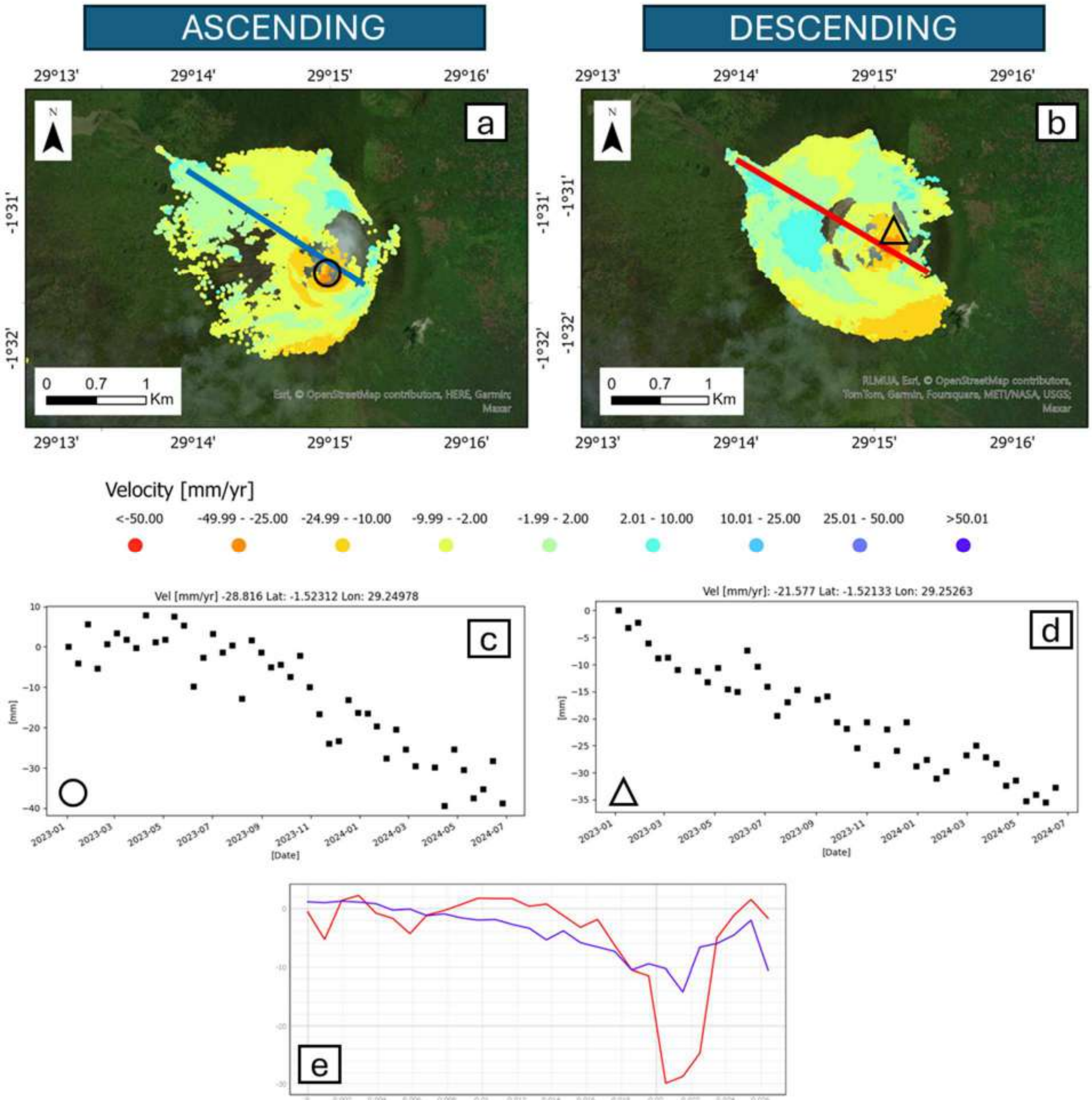

Figure 37. Line-of-sight velocity maps of the Nyiragongo volcano along the ascending orbit (a) and the descending orbit (b) and their respective time series (c, d) utilizing Sentinel-1 data spanning the time period from January 2023 to July 2024. Velocity profiles crossing the volcanic crater for the ascending orbit in blue and descending orbit in red (e).

A deformation pattern is identified in the city of Goma, on both the ascending and the descending orbit data (Figure 38a and Figure 38b). The pattern consists of a few areas elongated about N-S, characterised by negative (-3 to -5 mm/yr) and positive (+4 to +7 mm/yr) velocities. These zones appear to be distributed along the E-W direction, creating strong velocity gradients (about 10 mm/yr over 5 km), whose direction depends on the Line of Sight of the map. The N-S elongation follows the general direction of active geological structures, as the dike which was modelled during the 2021 eruption or the active fault structure mapped in the GEM active fault database: https://www.globalquakemodel.org/product/active-faults-database.

These results must be considered preliminary and further analysis must be performed to better investigate any correlation between the volcanic and tectonic structures and the deformation patterns.

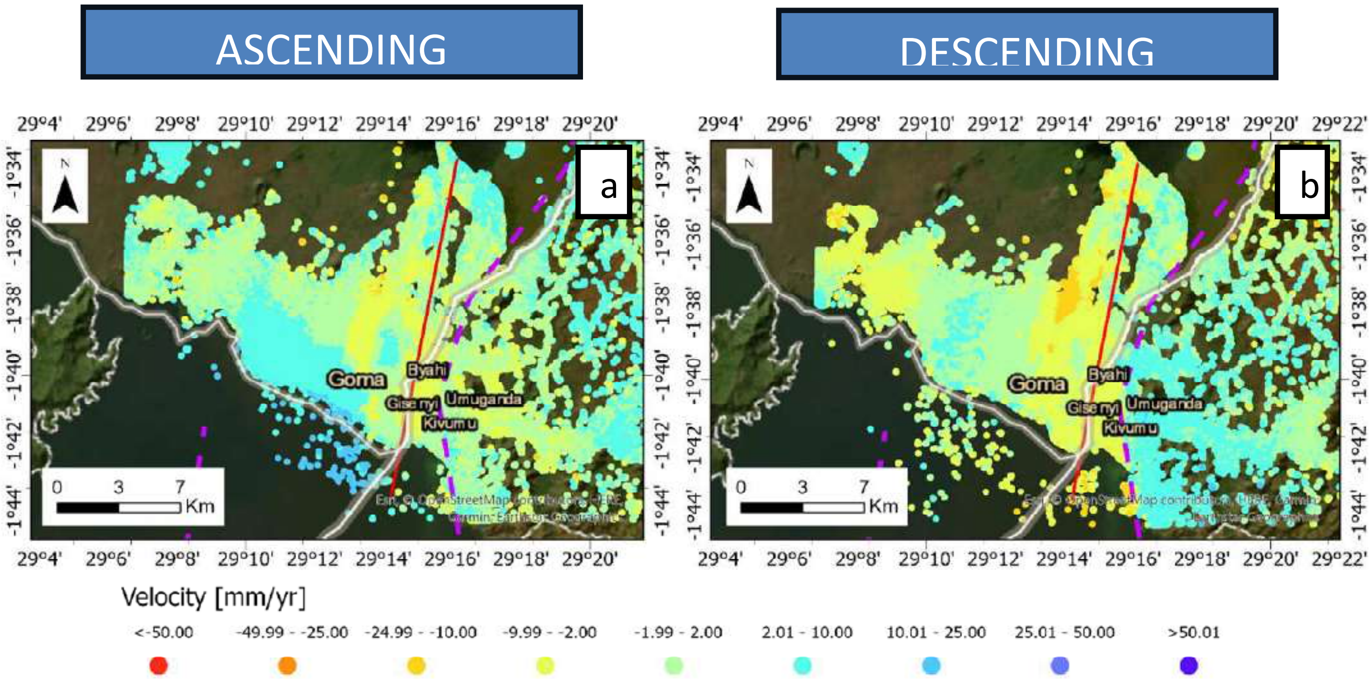

Figure 38. Line-of-sight velocity maps of the city of Goma along the ascending orbit (a) and the descending orbit (b) of Sentinel-1 data spanning the time period from January 2023 to July 2024. The purple dashed lines represent the fault system. The red solid line identifies the trace of the 2021 modelled dike

3.2. Nyamulagira volcano

The IPTA expend deformation rate map of the Nyamulagira volcano shows mainly negative velocities inside the crater, with values around -25 mm/yr. There is also negative velocity along the NW flank of the volcano, associated to the compaction of the May 2023 lava flows.

Inside the crater the displacement time series show that the ground has been lowering around 100 mm since the inception of the small May 2023 eruption (Figure 39).

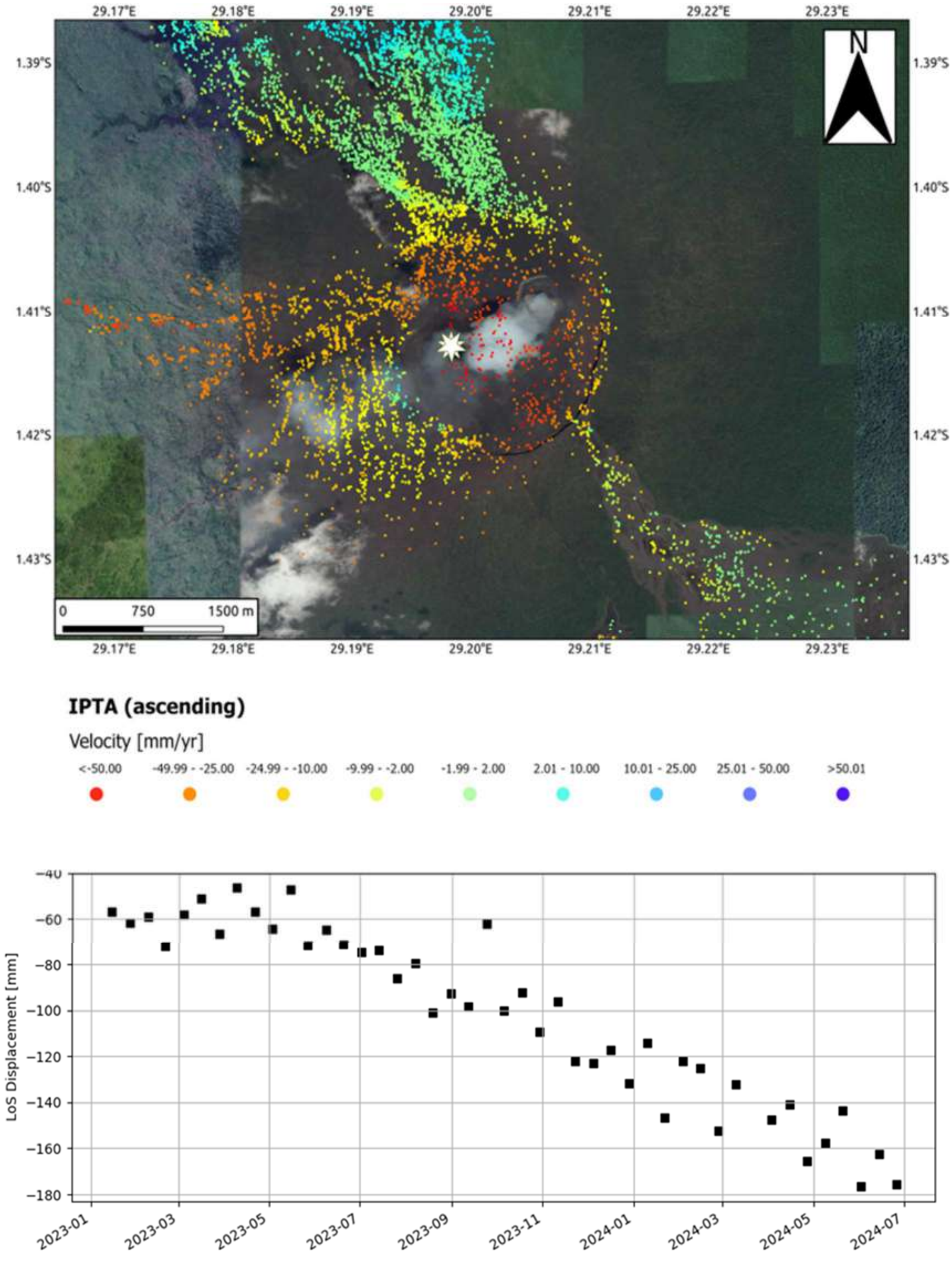

Figure 39. *Ascending deformation rate map of the Nyamuragira volcano and the respective time series plot for points inside the main crater.*

5.2.3. Assessment of recent ground deformations of Nyiragongo and Nyamulagira volcanoes using COSMO-SkyMed data

1. Introduction

The Virunga volcanic region is characterized by complex topography, dense vegetation, and significant atmospheric disturbances, all of which contribute to severe temporal decorrelation in SAR interferometry. To overcome these challenges and map volcano-induced ground deformation, we employed the multi-temporal Small BAseline Subset (SBAS) approach. This analysis leveraged ascending and descending datasets from both the first- and second-generation COSMO-SkyMed missions, covering the period from October 2022 to December 2024.

2. Data and Methods

The area of interest (AOI) was monitored using COSMO-SkyMed ascending and descending orbits. The applied multi-temporal algorithm was SBAS (Lanari et al., 2004), as implemented in the SARscape software. The output maps have been geocoded at a spatial resolution of 30 m. The area of interest considered for the SBAS is shown in Figure 40.

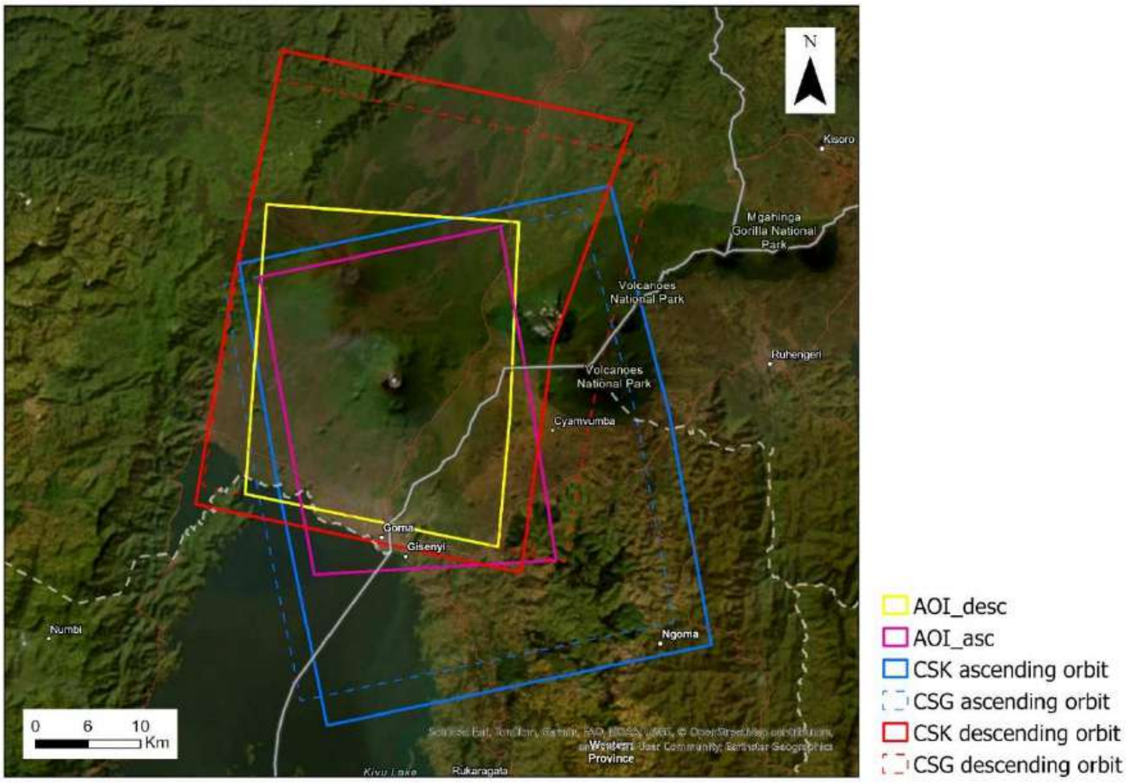

Figure 40. Overview of the study area. The footprints of the first- and second-generation COSMO-SkyMed missions are shown as solid and dashed polygons, respectively. Light blue indicates ascending orbits, while red denotes descending orbits. The yellow and purple polygons highlight the areas processed using SBAS algorithms.

The characteristics of the COSMO-SkyMed datasets used are reported in Table 2.

Table 2. Characteristics of the processed COSMO-SkyMed datasets

Orbit	Ascending	Descending
Platform	CSK and CSG	CSK and CSG
No. of images	161	145
Data Product	Single Look Complex (SLC)	Single Look Complex (SLC)
Acquisition Mode	HIMAGE/STIPMAP	HIMAGE/STIPMAP
Start Date	20221018	20221109
End Date	20241224	20241207

3. Results

Figure 41 presents ascending and descending MT-InSAR LoS velocity maps together with the corresponding displacement time series extracted at selected points. In the velocity maps, red colors indicate motion away from the satellite, whereas blue colors indicate motion toward the satellite. The resulting velocity maps reveal generally stable conditions across most of the study area, with the exception of Goma city, which exhibits a positive deformation trend characterized by uplift velocities (Figure 41a). A pronounced negative deformation pattern is also visible in both geometries (Figure 41a and 41b), with LoS velocities reaching up to −20 mm/yr. This signal may be associated with the deflation process that followed the dyke intrusion related to the May 22, 2021 eruption of Nyiragongo volcano.

The displacement time series confirm a progressive and nearly linear deformation trend throughout the observation period. In the ascending dataset, the point marked by the black star exhibits a mean LoS velocity of approximately 3.3 mm/yr, whereas the blue-circled point shows stronger deformation, reaching about −10 mm/yr. The descending time series indicates a LoS velocity of approximately −8.8 mm/yr at the selected location (red circle). The consistency between ascending and descending observations suggests persistent ground deformation affecting the monitored area.

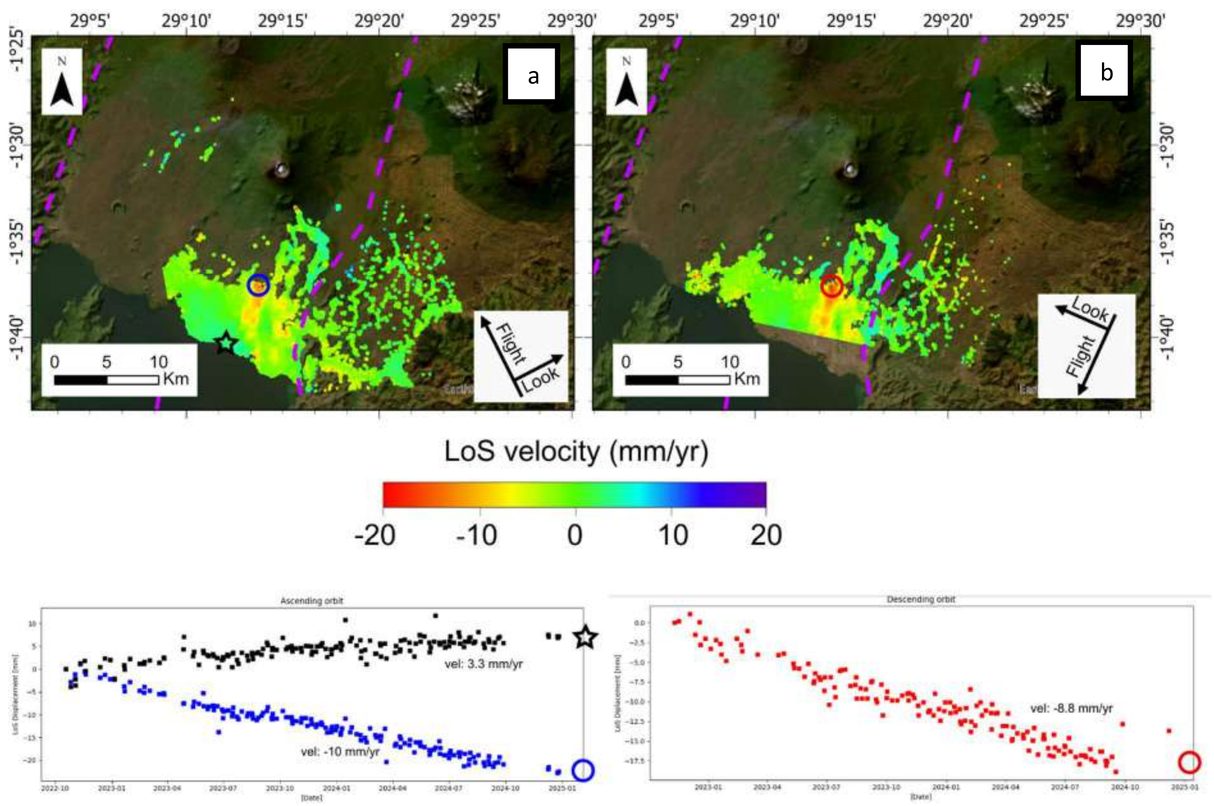

Figure 41. MT-InSAR LOS deformation velocity maps derived from (a) ascending and (b) descending satellite orbits. Red colors indicate motion away from the satellite, whereas blue colors indicate motion toward the satellite. The dashed purple line marks the main faults extracted from the GEM database. The lower panels show the displacement time series extracted at the selected points highlighted by the black star, blue circle, and red circle, together with the corresponding average LOS velocities (mm/yr).

5.2.4. Contribution of the satellite monitoring system MOUNTS to the surveillance of Nyiragongo and Nyamulagira volcanoes (DRC) during 2024 and 2025

1. MOUNTS monitoring system

MOUNTS (Monitoring Unrest from Space, www.mounts-project.com, Valade et al., 2019) is a satellite-based volcano monitoring system, exploiting the diversity of sensors on-board the polar-orbiting Sentinel spacecrafts (ESA Copernicus). The synergistic use of radar (Sentinel-1 SAR), short-wave infrared (Sentinel-2 MSI) and ultraviolet (Sentinel-5P TROPOMI) payloads allow for surveillance of surface deformation, emplacement of volcanic deposits, detection of thermal anomalies, and emission of volcanic SO_2 (Figure 42).

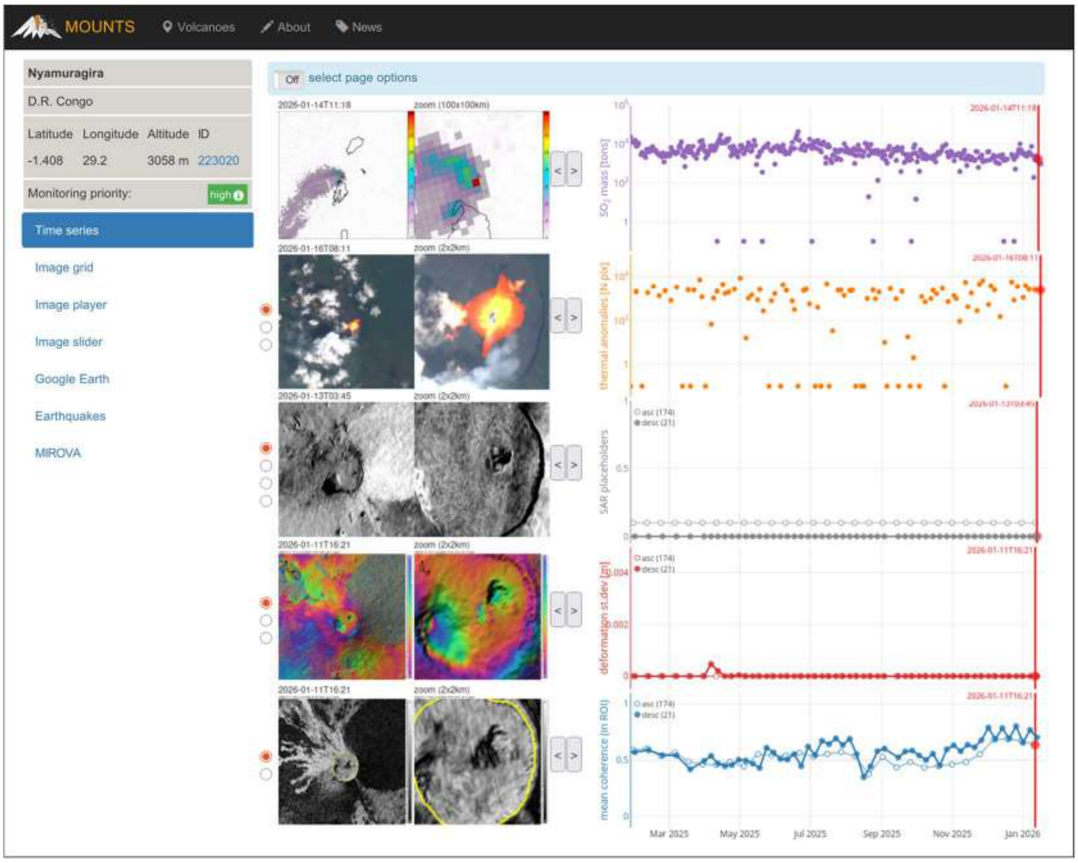

Figure 42. Screenshot of the MOUNTS web interface (http://www.mounts-project.com) showing the monitoring of Nyamuragira volcano through Sentinel-5P (SO_2 mass in purple), Sentinel-2 (hot pixels in orange, Massimetti et al., 2020), and Sentinel-1 (SAR amplitude in gray, INSAR displacement in red, InSAR coherence in blue).

Deep Learning "plugins" are incorporated to assist specific processing tasks, such as the automatic detection of large deformation in InSAR interferograms (Valade et al. 2019) and SAR speckle filtering (Davis et al., 2020). Volcanic activity is visualized through the systematic display of geo-referenced images and time-series of the above-mentioned parameters at several tens of active volcanoes worldwide.

2. SO_2 emission from Virunga volcanoes

Following the drainage of Nyiragongo's lava lake in May 2021, SO_2 emissions from the Virunga volcanoes dropped significantly. From late 2023 through 2024, major changes in SO_2 emission rates were observed at the Kivu volcanoes Nyamuragira and Nyiragongo, with SO_2 levels increasing from values close to TROPOMI's detection limit, to extremely high values >10 kt (Figure 43).

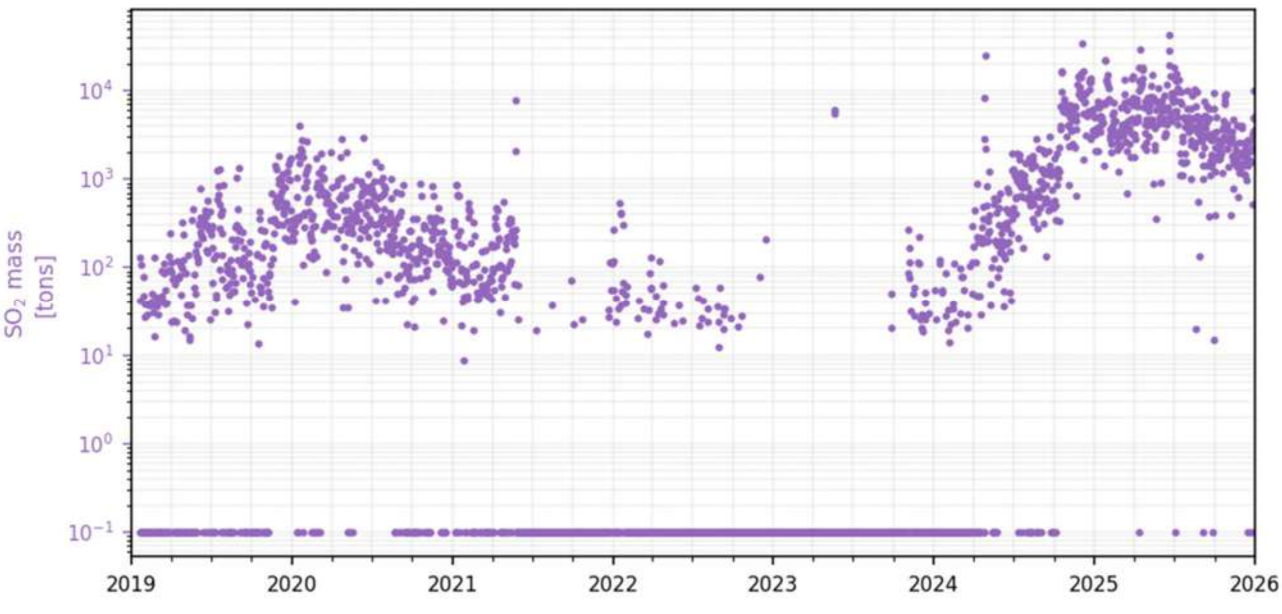

Figure 43. *SO_2 masses computed from Sentinel-5P TROPOMI images, in a 500x500 km region around Nyiragongo, representing the bulk emission from Virunga volcanoes.*

OMI images covering the entire year 2024, during which most of the observed changes occurred, were processed to derive monthly SO_2 fluxes following the method of Campion, 2014. In addition, a limited number of TROPOMI images were analyzed to better constrain daily SO_2 flux estimates. The monthly averaged SO_2 flux increased from approximately 150 t d^{-1} to more than 10,000 t d^{-1} (Figure 44).

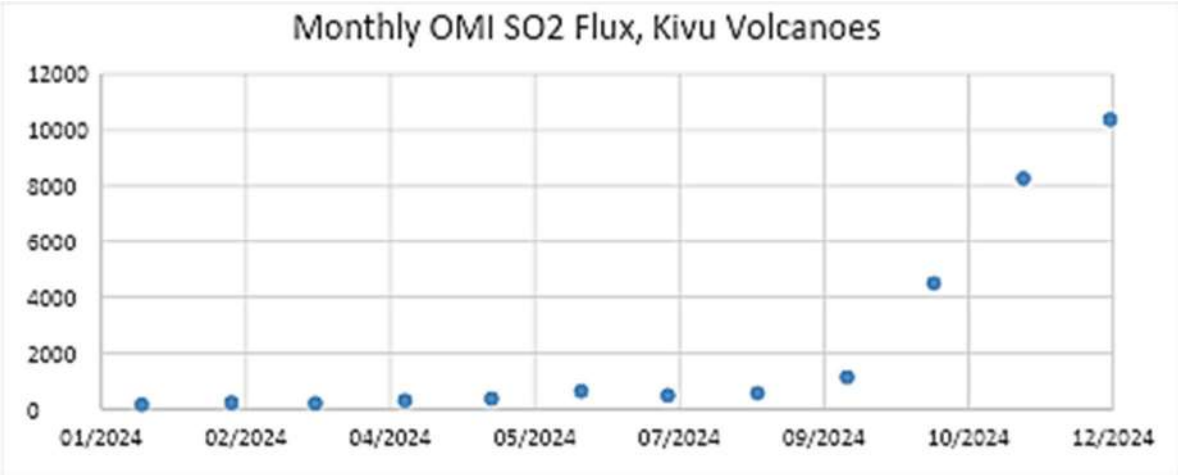

Figure 44. Evolution *of the monthly averaged SO_2 flux during 2024, derived from OMI images.*

The two previous periods of sustained high SO_2 flux were associated with the early stages of lava lake formation at Nyiragongo (2002–2003) and Nyamuragira (2012–2014). These episodes were likely linked to the initial degassing of newly accumulated magma batches that subsequently fed the long-lived lava lakes at both volcanoes (Campion and Coppola, 2023). The spatial resolution of TROPOMI imagery is generally insufficient to reliably separate SO_2 plumes from Nyiragongo and Nyamuragira volcanoes. Only under rare conditions (when the plumes are narrow and oriented predominantly towards the SW or NE) can the relative contribution of each volcano be crudely estimated (Figure 45a). To complement this analysis, we performed a qualitative analysis of the images of the ASTER (Advanced Spaceborne Thermal Emission and Reflection Radiometer) sensor, which have a resolution of 90 m in the thermal InfraRed (TIR), Figure 45b-c. These images confirm that the dimensions and concentrations of the SO_2 plumes of Nyamuragira and Nyiragongo are of the same order of magnitude, so that their respective emissions rates are roughly similar.

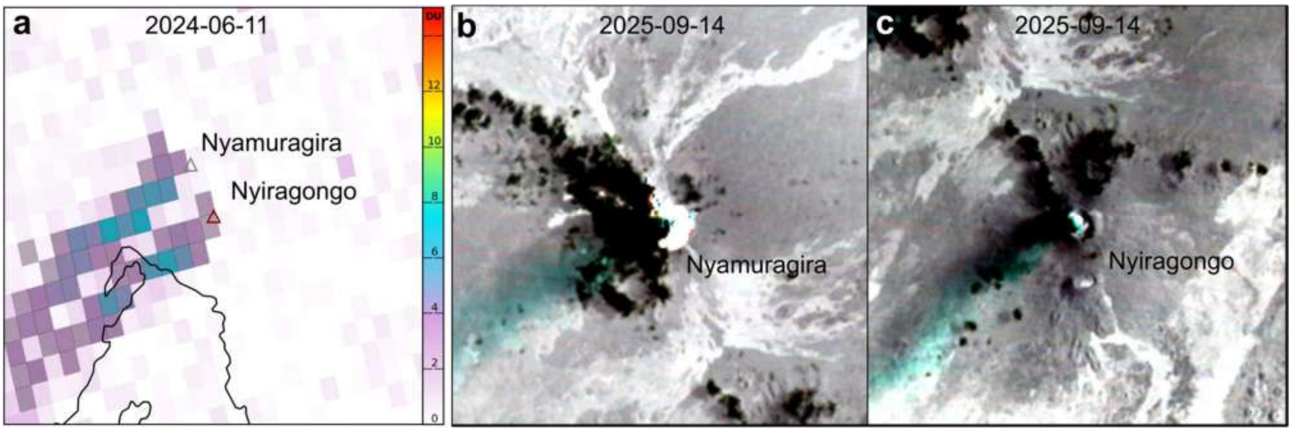

Figure 45. *a) MOUNTS image of Sentinel-5P Tropomi SO_2 distribution from Virunga Volcanoes, on 11/06/2024. b) ASTER_TIR images of Nyamuragira and c) of Nyiragongo on 14/09/2025. These are Pseudocolor images obtained by assigning Bands 11, 13 and 14 of ASTER to an RGB linear stretching over the image range dynamics. SO_2 absorption on band 11 (centered at 8.5 µm) produces the distinctive cyan hue of the gas plumes.*

3. Nyiragongo

The May 2021 eruption of Nyiragongo was followed by a drastic reduction in the SO_2 emissions and thermal anomalies, consistent with the drainage of the summit lava lake. In the days following the onset, Sentinel-1 SAR images showed a fast collapse of the crater, evidenced by an increased size and depth of the bottom-most pit crater (see 2022 in Virunga Supersite Biennal Report 2020-2021 after Balagizi et al., 2022). Analysis of the Sentinel-1 SAR images allow recovery of the depth's variations of both lava lakes and/or pit crater. This is done by measuring the length of the shadow cast by the crater walls in radar geometry, and multiplying it by the cosine of the radar incidence angle (Wadge et al., 2011). The method has been applied to track lava lake level variations at Nyiragongo (Barrière et al., 2022, 2018) and Erta Ale (Moore et al., 2019), and at Nyamuragira it has been applied by MOUNTS to provide variations of the pit-crater floor (Burgi et al., 2021). Analysis of Sentinel-1 images at Nyiragongo reveals the collapse that occurred in May 2021 following the drainage of the lava lake (Figure 46, red arrow), as well as the subsequent slow refilling of the crater (previously reported by Valade (2024) in the Virunga Supersite Biennal Report 2022-2023). Between June 2021 and January 2026, the crater floor rose by approximately 100 m. Inspection of Sentinel-2 images (Figure 46, inset) indicates that this progressive infilling is associated with successive episodes of small intra-crater lava flows. An acceleration of the crater infilling rate was observed from April to July 2024, coinciding with the onset of a dramatic increase in SO_2 masses detected by MOUNTS.

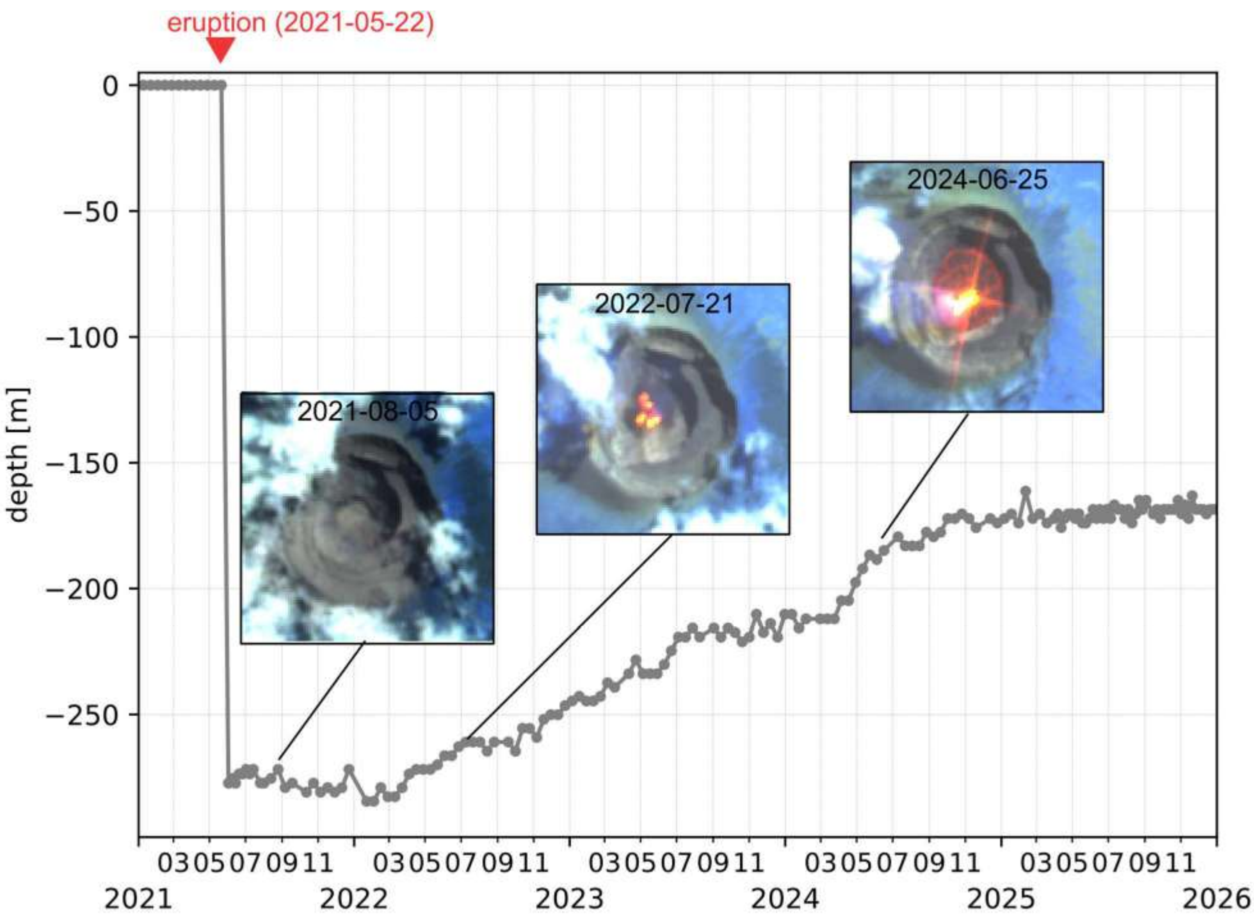

Figure 46. Analysis of Sentinel-1 products (descending orbit) showing the crater collapse in the days following the 2021 eruption onset, and the progressive crater infilling in the following years. Inset images are Sentinel-2 images (SWIR band composition) which suggest that this infilling is caused by successive lava flows inside the crater.

4. Nyamulagira

Much like the analysis presented for Nyiragongo, analysis of Sentinel-1 SAR images allows recovery of the changes in the floor depth of Nyamuragira's pit crater and main caldera. Figure 47a shows that during the 2024–2025 period the main caldera floor continued to infill, albeit at a moderate rate. In contrast, Figure 47b indicates that over the same period the pit crater did not exhibit any emptying or refill episodes. This contrasts with earlier periods documented by

(Burgi et al., 2021), and in MOUNTS contributions by Valade in the 2020–2021 and 2022–2023 Virunga Supersite Biennial Reports, during which multiple pit crater floor fluctuations were observed.

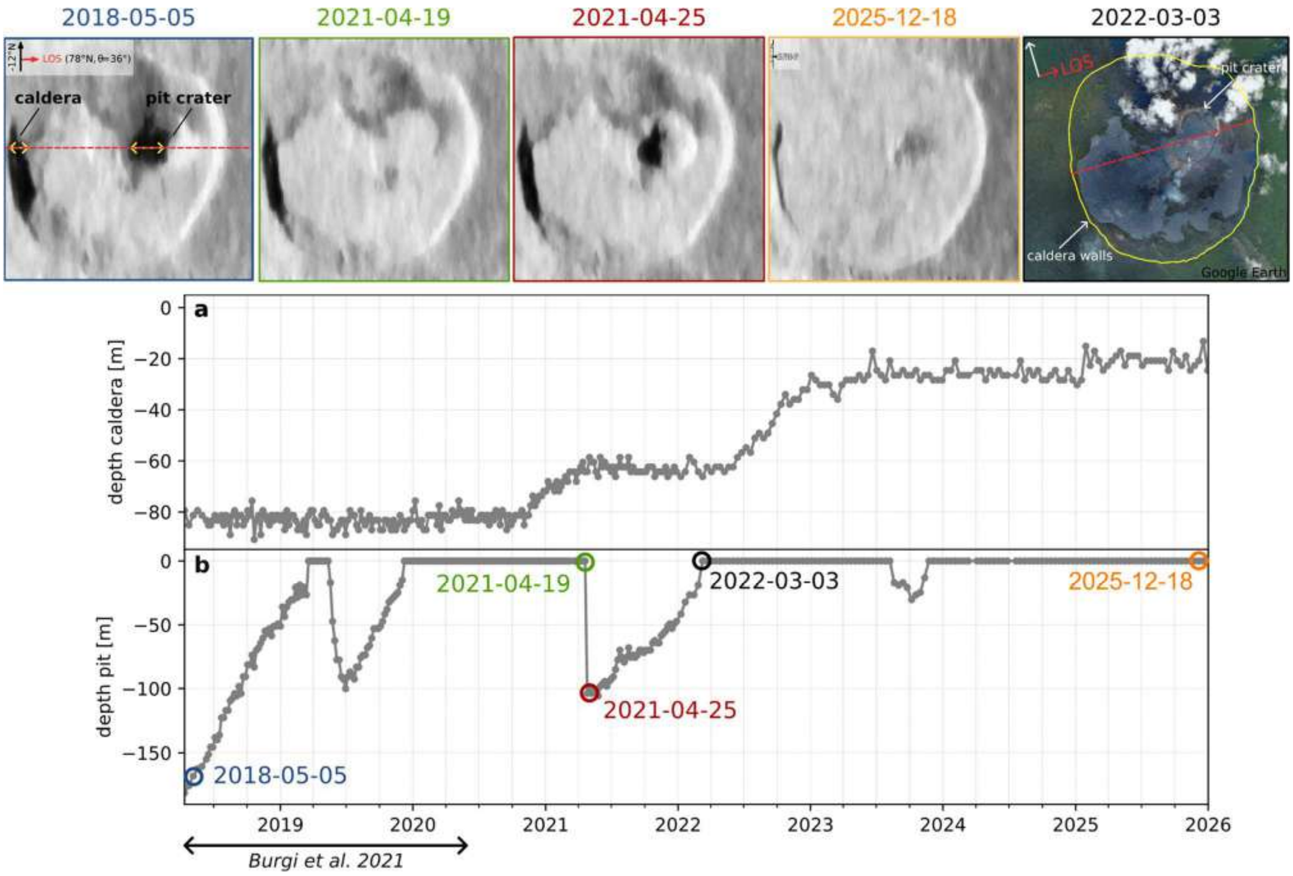

Figure 47. Variations of (a) the main caldera floor and (b) the pit crater floor at Nyamuragira during the period from 2018/04 to 2026/01, analyzed by MOUNTS from Sentinel-1 images. Top-row images: Sentinel-1 SAR images (ascending orbit 174) in radar geometry; yellow arrows indicate the SAR shadow used to recover depths of both the caldera floor and pit crater floor along the radar Line of Sight (LOS). Top-row right-most image: high-resolution optical image acquired on 2022-03-03 (Google Earth), dashed red line indicates the radar LOS along which the depths were calculated.

The continued infill of the main caldera by overflows from the pit crater continued to facilitate lava flows to overflow outside the caldera walls onto the slopes of the edifice, as observed from InSAR coherence maps and SWIR band compositions (Figure 47). Episodes of intense lava overflows spreading across the caldera are evidenced by a decrease in the mean coherence calculated over the caldera surface (Figure 48a; Polcari et al., 2024). The increased number of detected hot pixels reflects both intense intra-caldera lava overflows and lava flows extending beyond the caldera onto the volcano’s flanks (Figure 48a-b).

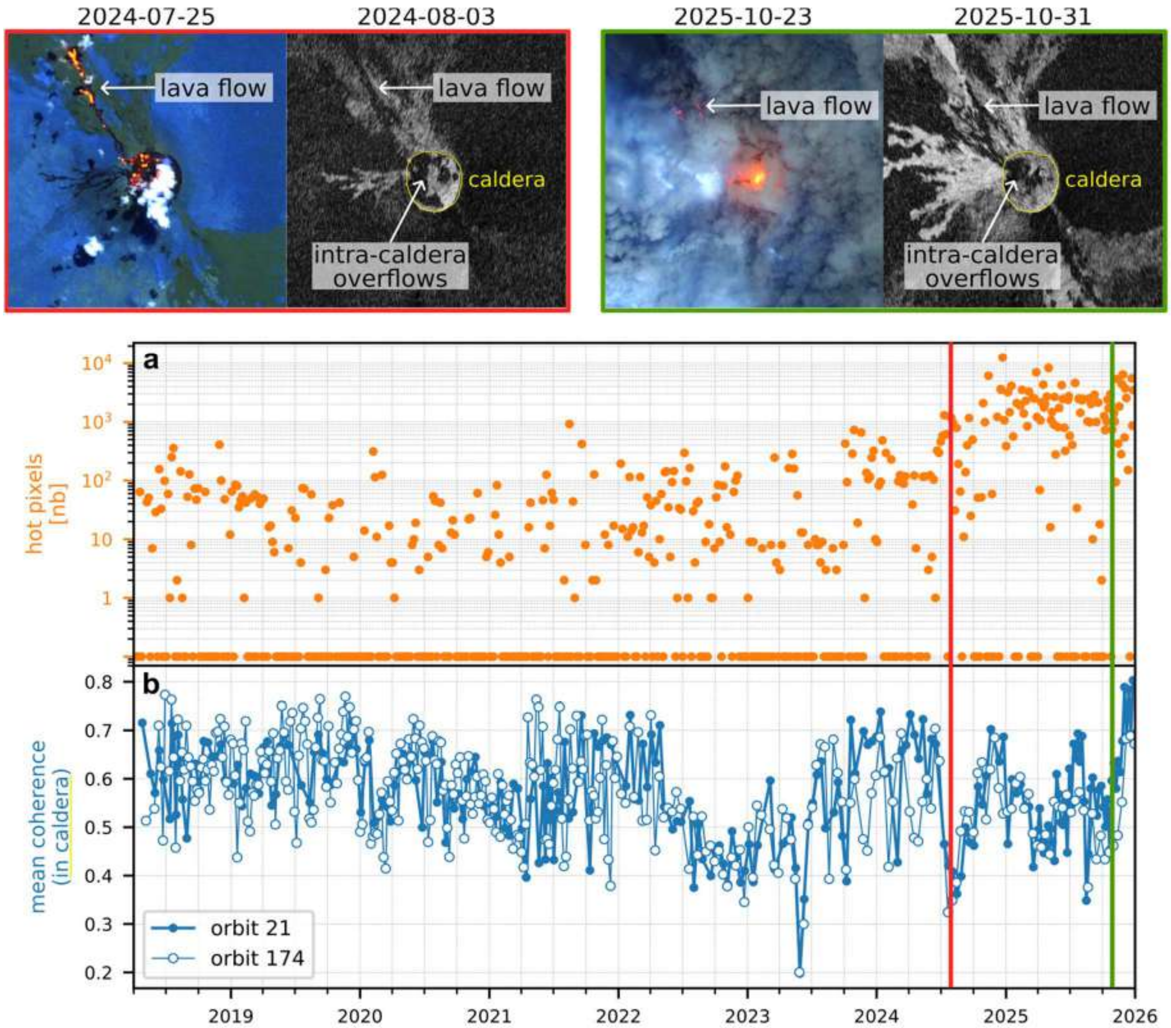

Figure 48. Nyamuragira: (a) hot pixels detected from Sentinel-2 imagery within a 10 × 10 km region, and (b) mean Sentinel-1 InSAR coherence within the caldera (outlined in yellow in the geocoded coherence images). The top row illustrates two episodes of pronounced intra-caldera overflows and lava flows, identified using Sentinel-2 SWIR band composites and Sentinel-1 InSAR coherence, and marked by red and green vertical lines.

Funding

The development of MOUNTS was funded by Geo.X (Research Network for Geosciences in Berlin and Potsdam) from 2017 to 2019, supported by UNAM PAPIIT funding (IA102221) from January 2021 to January 2023, and has been supported since January 2025 by UNAM PAPIIT funding under the "OMEGA" project (IN114625).

5.2.5. Thermal activity at Nyiragongo and Nyamulagira volcanoes (DRC) detected by the MIROVA system: 2024-2025

In this short report I summarize the satellite thermal observations made by the MIROVA system on the Nyiragongo and Nyamulagira volcanoes during 2024-2025. All data are visible on the website: https://www.mirovaweb.it/NRT/

1. Nyiragongo volcano:

During 2024-2025, Nyiragongo's thermal activity was persistent but variable (Figure 49a), always localized within the summit crater (Figure 49b). Between January and May 2024, the VRP showed a clear increase, from Volcanic Radiative Power (VRP) values of 2-5 MW (January 2024) up to VRP values > 100 MW (May 2024), punctuated by short (< 1 day) and sudden increases that reached peaks of 500-1000 MW (Figure 49a).

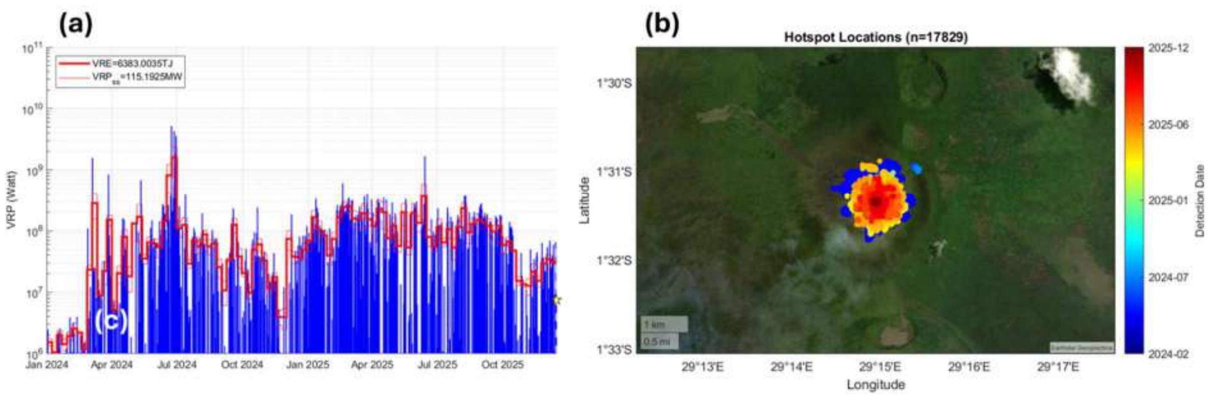

Figure 49. (a) Volcanic Radiative Power (VRP) recorded at Nyiragongo volcano by the MIROVA system (Coppola et al., 2020) during 2024-2025; (b) Location of thermal anomalies detected by Sentinel 2 and Landsat 8-9 over the same period using S2PIX algorithm (Massimetti et al., 2020).

A phase of more intense activity was recorded between June and July 2024, with VRP frequently > 1000 MW. Subsequently, the thermal flux showed a decreasing trend (VRP approximately 10 MW in December 2024) which reversed at the beginning of 2025. During 2025, thermal activity remained sustained at VRP of 100-500 MW and then decreased again to 10-20 MW starting from October 2025. We attribute this activity to a gradual, albeit oscillatory, process of reformation of the lava lake with fluctuations in the surface level and more or less intense spattering activity, possibly accompanied by intra-crater overflows. No thermal anomalies were observed outside the crater during the observed period (Figure 49b).

2. Nyamulagira volcano:

Throughout the 2024-2025 period, Nyamulagira's thermal activity (Figure 50a) was continuous and ranged in intensity from high (VRP > 100 MW) to very high (VRP > 1000 MW). Between January and March 2024, activity remained concentrated within the summit caldera, with VRP values between 100 and 300 MW. A sudden increase was recorded between 13 and 17 June, with VRP values exceeding 2000 MW, always localized in the crater area. This episode marks the beginning of a phase of intense thermal activity characterized by VRP values consistently exceeding 1000 MW, produced by intense intra-crater activity and numerous lava flows emplaced along the northwestern flank (Figure 50b). The lava flows extend for a maximum distance of 6-7 km and originate from the north-western sector of the caldera (Figure 49b; Figure 48). Overall, the measured VRP is sourced by two processes: (i) strong intra-crater activity associated with the presence of a lava lake, intense spattering and numerous intra-crater overflows that partially filled the caldera floor (Figure 51) and (ii) by numerous lava flows emerging from the north-western crater rim end extending up to 6-7 km from the crater rim (Figure 50b).

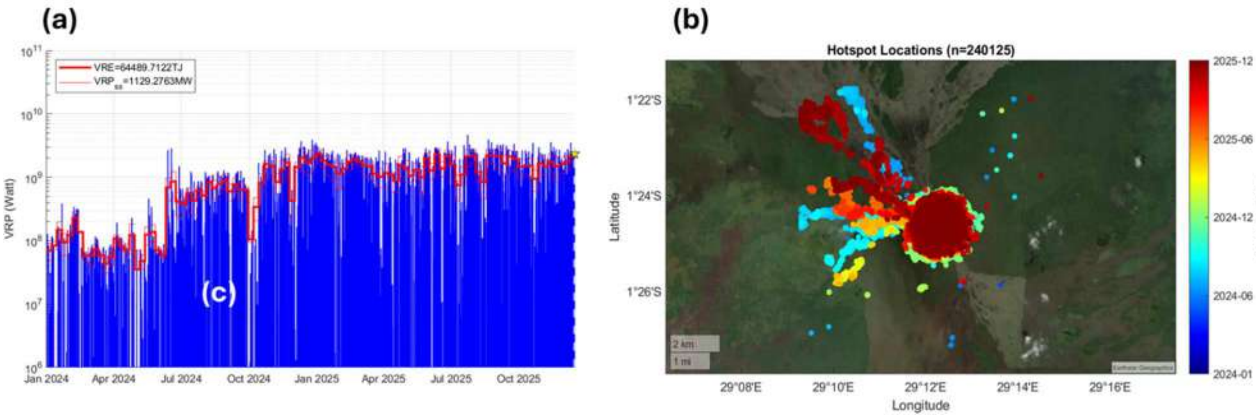

Figure 50. (a) Volcanic Radiative Power (VRP) recorded at Nyamuragira volcano by the MIROVA system (Coppola et al., 2020) during 2024-2025; (b) Location of thermal anomalies detected by Sentinel 2 and Landsat 8-9 over the same period using S2PIX algorithm (Massimetti et al., 2020).

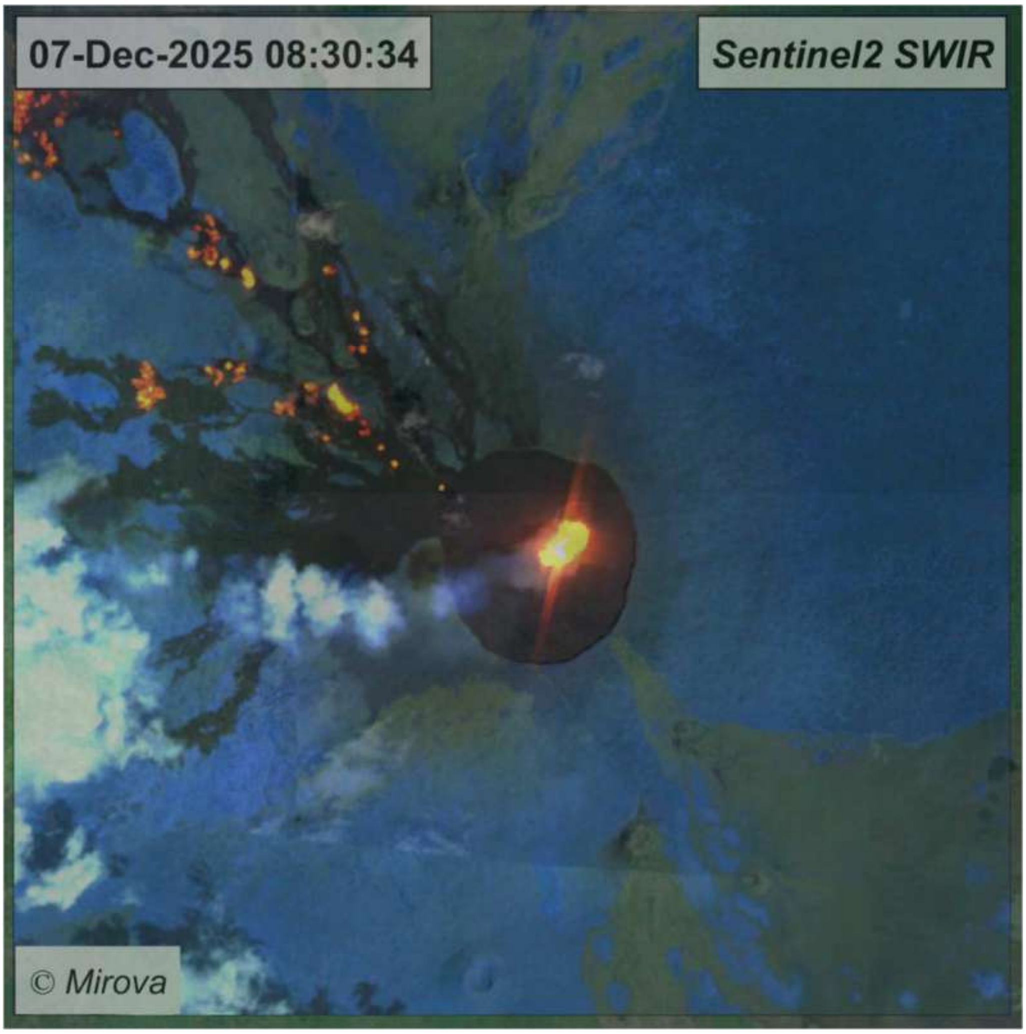

Figure 51. Immagine Sentinel 2 del 7 Dicembre 2025 (combinazione di bande B12-B11_B8A) che mostra le anomalie termiche associate all'attività intracraterica, ed effusiva lungo il fiango nord-occidentale del vulcan (https://www.mirovaweb.it/NRT/volcanoDetails_MSI.php?volcano_id=223020)

Publications

Peer reviewed journal articles

Charles M. Balagizi and Thérèse Mosange, 2025. Qualité de l'air dans la ville volcanique de Goma, Les Editions du Pangolin, ISBN n° 978-2-87467-172-2. Dépôt Légal n° 2025/9944/191 ; Belgium

Polcari M., Ferrentino E., Balagizi Charles, Coppola D., Valade S., 2025. 2023 activity of Nyamulagira volcano monitored by SAR interferometric coherence, Science of Remote Sensing, https://doi.org/10.1016/j.srs.2025.100261

Viveiros F., Elias T., Ilyinskaya E., Balagizi C., Stewart C., Ricci T, Joseph E. P., Hernández P. A., 2025. Volcanic gas impacts, Chapter 2.4 within PART 4 of The Encyclopedia of Volcanoes, 3rd ed., Elsevier. https://doi.org/10.31223/X5PB1F

Sadiki, A., Nzamu, S., Rusimbuka, M. et al. Challenges and resilience in monitoring the active volcanoes of the Virunga Chain: effects of political conflicts on scientific research and population safety in North Kivu, DR Congo. Bull Volcanol 87, 85 (2025). https://doi.org/10.1007/s00445-025-01846-9

Kyambikwa, A.A., Maombi, S., Sadiki, A. et al. The May 22nd 2021 eruption of Nyiragongo Volcano, DRC: field observations and reconstruction of eruption dynamics. Bull Volcanol 87, 88 (2025). https://doi.org/10.1007/s00445-025-01872-7

Balagizi., C.M., 2025. Virunga Supersite: improving volcano monitoring in a limited resource and conflict-laden zone. GEO Global Forum 2025, Roma-Italy.

Sadiki, A., Kyambikwa, A., Namogo, D., Diomi, L., Munguiko, O., et al. (2024). Analysis of the Seismicity Recorded Before the May 22, 2021 Eruption of Nyiragongo Volcano, Democratic Republic of the Congo. In SSA 2024 Annual Meeting Proceedings, Seismological Research Letters, 95(2B), 1113–1465. https://doi.org/10.1785/0220240136

Balagizi., C.M., 2025. Importance of satellite imagery for assessing and monitoring volcanic hazard in inaccessible sites: the case of Virunga volcanoes, DR Congo (East Africa). GEO Global Forum 2025, Roma-Italy.

Balagizi., C.M., 2025. TS2: No time to waste: The race for effective multi-hazard early warning systems in fragile and conflict settings. Global Platform for Disaster Risk Reduction, Génève 2 au 6 juin 2025.

Sadiki, A., Kyambikwa, A., Namogo, D., Diomi, L., Munguiko, O., Balezi , G., Sifa, L., Nzamu,S., Mashagiro, N., Balagizi, C., Mavonga, G., McCausland, W., Pre- and post-eruption seismicity associated with the May 2021 volcanic eruption at Nyiragongo and new appearance of lava lake in the main crater, 2024 Nemmers Workshop on volcano & rift seismicity in the branches of the East African Rift System, Northwestern University, Evanston, IL, May 2024.

Research products

All the research products listed in this report will be accessible at the GEO GNSL website, Virunga Supersite section at http://geo-gsnl.org/supersites/permanent-supersites/virunga-supersite/

Research product issues

Some research products and ground-based data are still currently not publicly released, as they remain under embargo to enable the scientific team to publish their findings. However, these results can be made available upon request for purposes related to hazard assessment and crisis management.

6. Dissemination and outreach

- Scientific products contained in this report have already been shared with local institutions engaged in hazard assessment activities, notably the Goma Volcano Observatory (GVO), which is responsible for the surveillance of the active volcanoes Mount Nyiragongo and Mount Nyamulagira and lake Kivu.
- The GVO Volcano Information Centre also used these products during the awareness-raising activities on volcanic risk prevention intended for university students and school pupils, as well as other Goma inhabitants.
- The products were also used in local and international conferences listed at the "publication section" of the present report.
- Training of local scientists:
  - Mr Albert Kyambikwa from GVO's department of seismology is taking a PhD in seismology at the department of Earth and Environmental Sciences, Tulane University in the USA.
  - Mr Gloire Sambo from GVO's department of geodesy had accomplished a one-year (October 2024 to October 2025) training in processing EO data (Interferometric Synthetic Aperture Radar and Thermal Anomaly Analysis) at INGV, branches of Roma and Catania.

- Mr Bonheur Ngangu from GVO's department of geodesy had accomplished a one-year (October 2024 to October 2025) training in processing GNSS data, as well as installing and maintaining at INGV, branch of Catania.
- Mr Marcellin Kasereka is taking a training in Geochemical techniques for active volcanoes monitoring at INGV Palermo, a training that will last one year.

7. Funding

The Virunga Supersite has no funding; all the activities were realized by scientists working on a voluntary basis.

8. Stakeholders interaction and societal benefits

The Goma Volcano Observatory (GVO) is still the main and direct beneficiary of the support, services and products provided by the Virunga Supersite. Most of these outputs are scientific-based and directly support volcanic research and monitoring activities, with the aim of improving the GVO's capacity to detect precursory unrest allowing this institution to forecast eruptions, issue timely warnings, and save lives. The products are incorporated into the routine operational framework of the GVO and contribute to the generation of information disseminated to stakeholders, including the weekly bulletin on volcanic activity levels, as well as other communications addressed to governmental authorities and the broader public, including students.

9. Conclusive remarks and suggestions for improvement

The Virunga Geohazards Supersite is presently an functioning scientific network composed of local and international scientists and institutions. International scientist and institutions have provided key training to a certain number of local scientists, and allowed access to important Earth Observation data for Nyiragongo and Nyamulagira volcanoes as well as the assessment of the related hazards. However, all these activities have been conducted on a voluntary basis on from donation. Hence, funding is strongly needed to support the deployment of instruments for ground-based data collection, enhancing local infrastructure, and facilitating the training and capacity-building of local scientists more local scientists and technicians, not only from GVO but from other local institutions.

10. Dissemination material for GEO/CEOS (discretionary)

All the materials included in this report can be utilized by the CEOS and the GEO for the dissemination.

11. References

Arellano, S., Yalire, M., Galle, B., Bobrowski, N., Dingwell, A., Johansson, M., Norman, P., 2017. Long-term monitoring of SO2 quiescent degassing from Nyiragongo's lava lake. Journal of African Earth Sciences 134, 866–873. https://doi.org/10.1016/j.jafrearsci.2016.07.002

Balagizi, C., 2016. Water geochemical investigation in the Nyiragongo and Nyamulagira volcanic fields: implications for Lake Kivu water chemistry (PhD Thesis). SECONDA UNIVERSITÀ DEGLI STUDI DI NAPOLI, Italy.

Balagizi, C., Mashagiro, N., Kasereka, M., Kelly, P., 2023. Pre- and post-eruptive gas composition measurements at Nyiragongo Volcano, East Africa, using a portable Multi-GAS (other). display. https://doi.org/10.5194/egusphere-egu23-16823

Balagizi, C., Mavonga, G., Kasereka, M., Liotta, M., Mariarosaria Manzo, Lanari, R., Bonano, M., Luca, C.D., Onorato, G., Jeanpy Lukindula, Ganci, G., Negro, C.D., Cappello, A., Coltelli, M., Mattia, M., Coppola, D., Durrheim, R.J., Mukambilwa, P., Kyambikwa, A., Niche Mashagiro, Ciraba, H., Lowenstern, J.B., Kelly, P.J., McCausland, W., Kies, A., 2020. Virunga Volcanoes Supersite Biennial Report: 2017- 2019. Zenodo. https://doi.org/10.5281/ZENODO.3911065

Balagizi, C., Mavonga, G., Kyambikwa, A., Sadiki, A., Ciraba, H., Iragi, K., Kavuke, J., Nzamu, S., Bonheur Ngangu, Niche Mashagiro, Kasereka, M., Safari, F., Rusimbuka, M.B., Habiyakare, T., Tite Niyitegeka, Galle, B., Poland, M., Liotta, M., Aoki, Y., Nobile, A., Ganci, G., Cappello, A., Proietti, C., Kolzenburg, S., Borgstrom, S., Mattia, M., Privitera, E., Coltelli, M., Valade, S., Coppola, D., Kelly, P., Griswold, J.P., Tolomei, C., Beccaro, L., Trasatti, E., 2022. Virunga Volcanoes Supersite Biennial Report: 2020- 2021. Zenodo. https://doi.org/10.5281/ZENODO.6338729

Balagizi, C.M., Darchambeau, F., Bouillon, S., Yalire, M.M., Lambert, T., Borges, A.V., 2015. River geochemistry, chemical weathering, and atmospheric C O $_2$ consumption rates in the V irunga V olcanic P rovince (E ast A frica). Geochem Geophys Geosyst 16, 2637–2660. https://doi.org/10.1002/2015GC005999

Balagizi, C.M., Kasereka, M.M., Cuoco, E., Liotta, M., 2018a. Influence of moisture source dynamics and weather patterns on stable isotopes ratios of precipitation in Central-Eastern Africa. Science of The Total Environment 628–629, 1058–1078. https://doi.org/10.1016/j.scitotenv.2018.01.284

Balagizi, C.M., Kasereka, M.M., Cuoco, E., Liotta, M., 2017. Rain-plume interactions at Nyiragongo and Nyamulagira volcanoes and associated rainwater hazards, East Africa. Applied Geochemistry 81, 76–89. https://doi.org/10.1016/j.apgeochem.2017.03.018

Balagizi, C.M., Kasereka, M.M., Kyambikwa, A.M., Cuoco, E., Arienzo, I., Liotta, M., 2022. Characterizing groundwater recharge sources using water stable isotopes in the North Basin of Lake Kivu, East Africa. Chemical Geology 594, 120778. https://doi.org/10.1016/j.chemgeo.2022.120778

Balagizi, C.M., Kies, A., Kasereka, M.M., Tedesco, D., Yalire, M.M., McCausland, W.A., 2018b. Natural hazards in Goma and the surrounding villages, East African Rift System. Nat Hazards 93, 31–66. https://doi.org/10.1007/s11069-018-3288-x

Balagizi, C.M., Yalire, M.M., Ciraba, H.M., Kajeje, V.B., Minani, A.S., Kinja, A.B., Kasereka, M.M., 2016. Soil temperature and CO2 degassing, SO2 fluxes and field observations before and after the February 29, 2016 new vent inside Nyiragongo crater. Bull Volcanol 78, 64. https://doi.org/10.1007/s00445-016-1055-y

Barrière, J., d'Oreye, N., Oth, A., Geirsson, H., Mashagiro, N., Johnson, J.B., Smets, B., Samsonov, S., Kervyn, F., 2018. Single-Station Seismo-Acoustic Monitoring of Nyiragongo's Lava Lake Activity (D.R. Congo). Front. Earth Sci. 6, 82. https://doi.org/10.3389/feart.2018.00082

Barrière, J., Nicolas d'Oreye, Smets, B., Oth, A., Delhaye, L., Subira, J., Mashagiro, N., Derauw, D., Smittarello, D., Syavulisembo, A.M., Kervyn, F., 2022. Intra-Crater Eruption Dynamics at Nyiragongo (D.R. Congo), 2002–2021. JGR Solid Earth 127, e2021JB023858. https://doi.org/10.1029/2021JB023858

Bobrowski, N., Giuffrida, G.B., Yalire, M., Lübcke, P., Arellano, S., Balagizi, C., Calabrese, S., Galle, B., Tedesco, D., 2017. Multi-component gas emission measurements of the active lava lake of Nyiragongo, DR Congo. Journal of African Earth Sciences 134, 856–865. https://doi.org/10.1016/j.jafrearsci.2016.07.010

Burgi, P.-Y., Valade, S., Coppola, D., Boudoire, G., Mavonga, G., Rufino, F., Tedesco, D., 2021. Unconventional filling dynamics of a pit crater. Earth and Planetary Science Letters 576, 117230. https://doi.org/10.1016/j.epsl.2021.117230

Campion, R., 2014. New lava lake at Nyamuragira volcano revealed by combined ASTER and OMI SO_2 measurements. Geophysical Research Letters 41, 7485–7492. https://doi.org/10.1002/2014GL061808

Campion, R., Coppola, D., 2023. Classification of lava lakes based on their heat and SO2 emission: Implications for their formation and feeding processes. Front. Earth Sci. 11, 1040199. https://doi.org/10.3389/feart.2023.1040199

Coppola, D., Campion, R., Laiolo, M., Cuoco, E., Balagizi, C., Ripepe, M., Cigolini, C., Tedesco, D., 2016a. Birth of a lava lake: Nyamulagira volcano 2011–2015. Bull Volcanol 78, 20. https://doi.org/10.1007/s00445-016-1014-7

Coppola, D., Laiolo, M., Cigolini, C., Donne, D.D., Ripepe, M., 2016b. Enhanced volcanic hot-spot detection using MODIS IR data: results from the MIROVA system. SP 426, 181–205. https://doi.org/10.1144/SP426.5

Coppola, D., Laiolo, M., Cigolini, C., Massimetti, F., Delle Donne, D., Ripepe, M., Arias, H., Barsotti, S., Parra, C.B., Centeno, R.G., Cevuard, S., Chigna, G., Chun, C., Garaebiti, E., Gonzales, D., Griswold, J., Juarez, J., Lara, L.E., López, C.M., Macedo, O., Mahinda, C., Ogburn, S., Prambada, O., Ramon, P., Ramos, D., Peltier, A., Saunders, S., De Zeeuw-van Dalfsen, E., Varley, N., William, R., 2020. Thermal Remote Sensing for Global Volcano Monitoring: Experiences From the MIROVA System. Front. Earth Sci. 7, 362. https://doi.org/10.3389/feart.2019.00362

Cuoco, E., Spagnuolo, A., Balagizi, C., De Francesco, S., Tassi, F., Vaselli, O., Tedesco, D., 2013a. Impact of volcanic emissions on rainwater chemistry: The case of Mt. Nyiragongo in the Virunga volcanic region (DRC). Journal of Geochemical Exploration 125, 69–79. https://doi.org/10.1016/j.gexplo.2012.11.008

Cuoco, E., Tedesco, D., Poreda, R.J., Williams, J.C., De Francesco, S., Balagizi, C., Darrah, T.H., 2013b. Impact of volcanic plume emissions on rain water chemistry during the January 2010 Nyamuragira eruptive event: Implications for essential potable water resources. Journal of Hazardous Materials 244–245, 570–581. https://doi.org/10.1016/j.jhazmat.2012.10.055

d'Oreye, N., González, P.J., Shuler, A., Oth, A., Bagalwa, L., Ekström, G., Kavotha, D., Kervyn, F., Lucas, C., Lukaya, F., Osodundu, E., Wauthier, C., Fernández, J., 2011. Source parameters of the 2008 Bukavu-Cyangugu earthquake estimated from InSAR and teleseismic data: Source parameters of 2008 Bukavu earthquake. Geophysical Journal International 184, 934–948. https://doi.org/10.1111/j.1365-246X.2010.04899.x

Darchambeau, F., Sarmento, H., Descy, J.-P., 2014. Primary production in a tropical large lake: The role of phytoplankton composition. Science of The Total Environment 473–474, 178–188. https://doi.org/10.1016/j.scitotenv.2013.12.036

Davis, T., Jain, V., Ley, A., D'Hondt, O., Valade, S., Hellwich, O., 2020. Reference-Free Despeckling of Synthetic-Aperture Radar Images Using a Deep Convolutional Network, in: IGARSS 2020 - 2020 IEEE International Geoscience and Remote Sensing Symposium. Presented at the IGARSS 2020 - 2020 IEEE International Geoscience and Remote Sensing Symposium, IEEE, Waikoloa, HI, USA, pp. 3908–3911. https://doi.org/10.1109/IGARSS39084.2020.9323293

Delvaux, D., Mulumba, J.-L., Sebagenzi, M.N.S., Bondo, S.F., Kervyn, F., Havenith, H.-B., 2017. Seismic hazard assessment of the Kivu rift segment based on a new seismotectonic zonation model (western branch, East African Rift system). Journal of African Earth Sciences 134, 831–855. https://doi.org/10.1016/j.jafrearsci.2016.10.004

Ebinger, C., Scholz, C.A., 2011. Continental Rift Basins: The East African Perspective, in: Busby, C., Azor, A. (Eds.), Tectonics of Sedimentary Basins. Wiley, pp. 183–208. https://doi.org/10.1002/9781444347166.ch9

Ebinger, C.J., 1989. Tectonic development of the western branch of the East African rift system. Geological Society of America Bulletin 101, 885–903. https://doi.org/10.1130/0016-7606(1989)101%3C0885:TDOTWB%3E2.3.CO;2

Halbwachs, M., Tietze, K., Lorke, A., Mudaheranwa, C., 2002. Investigations in Lake Kivu (east central Africa) after the Nyiragongo eruption of January 2002: Specific study of the impact of the sub-water lava inflow on the lake stability. Monogr. Solidarité, Paris.

Kasereka, M., YALIRE, M., MINANI, A., SAMBA, C.V., BISUSA, A.K., KAMATHE, E., MASHAGIRO, N., Muhindo SYAUSWA, KAVUKE, J., 2017. Les risques liés aux mazuku dans la région de Goma, république démocratique du Congo (Rift Est-Africain)." Journal of Water and Environmental Sciences 1(2): 164-174.

Kasereka, M.M., Cuoco, E., Zabene, F.Z., Balagizi, C.M., 2021. Baseline for rainwater chemistry and quality as influenced by Nyiragongo volcano permanent plume, East Africa. Chemosphere 283, 130859. https://doi.org/10.1016/j.chemosphere.2021.130859

Lanari, R., Mora, O., Manunta, M., Mallorqui, J.J., Berardino, P., Sansosti, E., 2004. A small-baseline approach for investigating deformations on full-resolution differential SAR interferograms. IEEE Trans. Geosci. Remote Sensing 42, 1377–1386. https://doi.org/10.1109/TGRS.2004.828196

Massimetti, F., Coppola, D., Laiolo, M., Valade, S., Cigolini, C., Ripepe, M., 2020. Volcanic Hot-Spot Detection Using SENTINEL-2: A Comparison with MODIS–MIROVA Thermal Data Series. Remote Sensing 12, 820. https://doi.org/10.3390/rs12050820

Mavonga, T., 2007. Some characteristics of aftershock sequences of major earthquakes from 1994 to 2002 in the Kivu province, Western Rift Valley of Africa. Tectonophysics 439, 1–12. https://doi.org/10.1016/j.tecto.2007.01.006

Mavonga, T., Durrheim, R.J., 2009. PROBABILISTIC SEISMIC HAZARD ASSESSMENT FOR THE DEMOCRATIC REPUBLIC OF CONGO AND SURROUNDING AREAS. South African Journal of Geology 112, 329–342. https://doi.org/10.2113/gssajg.112.3-4.329

Mavonga, T., Zana, N., Durrheim, R.J., 2010. Studies of crustal structure, seismic precursors to volcanic eruptions and earthquake hazard in the eastern provinces of the Democratic Republic of Congo. Journal of African Earth Sciences 58, 623–633. https://doi.org/10.1016/j.jafrearsci.2010.08.008

Moore, C., Wright, T., Hooper, A., Biggs, J., 2019. The 2017 Eruption of Erta ’Ale Volcano, Ethiopia: Insights Into the Shallow Axial Plumbing System of an Incipient Mid-Ocean Ridge. Geochem Geophys Geosyst 20, 5727–5743. https://doi.org/10.1029/2019GC008692

Sadiki, A.T., Kyambikwa, A.M., Namogo, D.B., Diomi, L.N., Munguiko, O.M., Balezi, G.M., Sifa, L.L., Nzamu, S.M., Mashagiro, N., Balagizi, C.M., Mavonga, G.T., 2023. Analysis of the Seismicity Recorded before the May 22, 2021 Eruption of Nyiragongo Volcano, Democratic Republic of the Congo. J. Volcanolog. Seismol. 17, 246–257. https://doi.org/10.1134/S0742046323700136

Smets, B., Kervyn, M., d’Oreye, N., Kervyn, F., 2015. Spatio-temporal dynamics of eruptions in a youthful extensional setting: Insights from Nyamulagira Volcano (D.R. Congo), in the western branch of the East African Rift. Earth-Science Reviews 150, 305–328. https://doi.org/10.1016/j.earscirev.2015.08.008

Tuluka, G.M., Lukindula, J., Durrheim, R.J., 2020. Seismic Hazard Assessment of the Democratic Republic of Congo and Environs Based on the GEM–SSA Catalogue and a New Seismic Source Model. Pure Appl. Geophys. 177, 195–214. https://doi.org/10.1007/s00024-018-2084-6

Valade, S., Ley, A., Massimetti, F., D’Hondt, O., Laiolo, M., Coppola, D., Loibl, D., Hellwich, O., Walter, T.R., 2019. Towards Global Volcano Monitoring Using Multisensor Sentinel Missions and Artificial Intelligence: The MOUNTS Monitoring System. Remote Sensing 11, 1528. https://doi.org/10.3390/rs11131528

Vaselli, O., Capaccioni, B., Tassi, F., YALIRE, M., 2003. The “Evil’s winds” (Mazukus) at Nyiragongo volcano (Democratic Republic of Congo). Acta Vulcanol. 14–15, 123-128.

Villeneuve, M., 1987. Géologie du synclinal de l’Itombwe (Zaïre oriental) et le problème de l’existence d’un sillon plissé pan-africain. Journal of African Earth Sciences (1983) 6, 869–880. https://doi.org/10.1016/0899-5362(87)90046-7

Villeneuve, M., Chorowicz, J., 2004. Les sillons plissés du Burundien supérieur dans la chaîne Kibarienne d’Afrique centrale. Comptes Rendus. Géoscience 336, 807–814. https://doi.org/10.1016/j.crte.2004.01.006

Wadge, G., Cole, P., Stinton, A., Komorowski, J.-C., Stewart, R., Toombs, A.C., Legendre, Y., 2011. Rapid topographic change measured by high-resolution satellite radar at Soufriere Hills Volcano, Montserrat, 2008–2010. Journal of Volcanology and Geothermal Research 199, 142–152. https://doi.org/10.1016/j.jvolgeores.2010.10.011

Wegmuller, U., Werner, C., 1997. Gamma SAR processor and interferometry software, Proceedings of the ERS Symposium on Space at the Service of Our Environment. ESA Publications Division: Florence, Italy.